Climate of the Past

Open Access

Peak glacial ^{14}C ventilation ages suggest major draw-down of carbon into the abyssal ocean

M. Sarnthein[1,3], B. Schneider[1], and P. M. Grootes[2]

[1]Institut für Geowissenschaften, University of Kiel, Olshausenstr. 40, 24098 Kiel, Germany
[2]Institute of Ecosystem Research, University of Kiel, Olshausenstr. 40, 24098 Kiel, Germany
[3]Institut für Geologie und Paläontologie, University of Innsbruck, 6020 Innsbruck, Austria

Correspondence to: M. Sarnthein (ms@gpi.uni-kiel.de)

Abstract. Ice core records demonstrate a glacial–interglacial atmospheric CO_2 increase of $\sim$ 100 ppm, while ^{14}C calibration efforts document a strong decrease in atmospheric ^{14}C concentration during this period. A calculated transfer of $\sim$ 530 Gt of ^{14}C-depleted carbon is required to produce the deglacial coeval rise of carbon in the atmosphere and terrestrial biosphere. This amount is usually ascribed to oceanic carbon release, although the actual mechanisms remained elusive, since an adequately old and carbon-enriched deep-ocean reservoir seemed unlikely. Here we present a new, though still fragmentary, ocean-wide Δ^{14}C data set showing that during the Last Glacial Maximum (LGM) and Heinrich Stadial 1 (HS-1) the maximum ^{14}C age difference between ocean deep waters and the atmosphere exceeded the modern values by up to 1500 ^{14}C yr, in the extreme reaching 5100 ^{14}C yr. Below 2000 m depth the ^{14}C ventilation age of modern ocean waters is directly linked to the concentration of dissolved inorganic carbon (DIC). We propose as a working hypothesis that the modern regression of DIC vs. Δ^{14}C also applies for LGM times, which implies that a mean LGM aging of $\sim$ 600 ^{14}C yr corresponded to a global rise of $\sim$ 85–115 μmol DIC kg^{-1} in the deep ocean. Thus, the prolonged residence time of ocean deep waters may indeed have made it possible to absorb an additional $\sim$ 730–980 Gt DIC, one third of which possibly originated from intermediate waters. We also infer that LGM deep-water O_2 dropped to suboxic values of <10 μmol kg^{-1} in the Atlantic sector of the Southern Ocean, possibly also in the subpolar North Pacific. The deglacial transfer of the extra-aged, deep-ocean carbon to the atmosphere via the dynamic ocean–atmosphere carbon exchange would be sufficient to account for two trends observed, (1) for the increase in atmospheric CO_2 and (2) for the 190 ‰ drop in atmospheric Δ^{14}C during the so-called HS-1 "Mystery Interval", when atmospheric ^{14}C production rates were largely constant.

1 Introduction

Global climatic and oceanic conditions underwent a series of fundamental transitions after the Last Glacial Maximum (LGM) that ended near 19 ka (Mix et al., 2001). These transitions comprised supposedly conflicting trends on land and in the ocean difficult to reconcile; thus they were named "Mystery Intervals" (details in Denton et al., 2006; Broecker and Barker, 2007). In particular, these problems apply to the period of North Atlantic meltwater stadial Heinrich 1 (HS-1), 17.5–14.7 ka.

Over the last years, the "mystery" became centered around the whereabouts of about 100 ppm of current atmospheric carbon during the LGM, considering the low-Δ^{14}C sources needed for the significant deglacial rise in atmospheric and terrestrial carbon of 200 Gt (Monnin et al., 2001) and 330–500 Gt (Ciais et al., 2012), respectively. This huge transfer of carbon needs to be reconciled with a simultaneous drop in atmospheric ^{14}C concentrations of $\sim$ 190 ‰. This problem is directly tied to questions regarding the state of the LGM deep ocean, the largest carbon reservoir of the surface Earth system, and to fundamental deglacial changes in ocean circulation that may have influenced it. These changes may have substantially controlled the ocean's capacity to store carbon.

Theoretical considerations and first evidence clearly suggest an enhanced LGM storage of carbon in the abyssal ocean (Archer and Winguth, 2000; Broecker, 1982; Bryan et al., 2010; Yu et al., 2010). However, box model results (Hain et al., 2011) and rough calculations on the basis of first abyssal ventilation ages (Broecker and Barker, 2007) suggested a series of potential major shortcomings in the concept that claims a reduced glacial Meridional Overturning Circulation (MOC) caused enhanced LGM storage. Thus the concept was rejected as quantitatively unreasonable in terms of radiocarbon budgets.

On the basis of box model experiments, Skinner (2009) proposed an expanded LGM volume of relatively cold and carbon-enriched deep waters analogous to the modern Circumpolar Deepwater. This mechanism would lead to an enlarged marine carbon inventory, supposedly without requiring "pre-imposed (deglacial) changes in (deep) ocean overturning rate". Alternatively, we now present empirical arguments for a new working hypothesis that assumes longer LGM mean transit times of deep waters in a constant deep-ocean volume and allows additional storage of ^{14}C-depleted carbon. In this context we assume a generally constant export productivity that can be explained by different time scales for the overturning of carbon and nutrients, as clearly shown by vertically decoupled fluxes of particulate organic carbon and nitrogen (Schneider et al., 2003).

To test the various model postulates and to quantify past changes in the carbon budget of the global ocean, we now combine modern oceanographic data with a set of modern and past *apparent ^{14}C ventilation ages* for ocean deep waters below 1500 m/2000 m water depth (w.d.) (Bard, 1998; Sarnthein, 2011; data sources in Table 1b and Fig. S1). These ages mean the time needed for a sample with pristine atmospheric ^{14}C concentration in surface waters to decay to the ^{14}C concentration observed in shallow- and deep-ocean samples, finally depicted in ^{14}C values of foraminifers. The age is called "apparent" because it is not a real age, since fluctuations in atmospheric ^{14}C concentration, ocean–atmosphere CO_2 exchange, and oceanic mixing processes co-determine the observed atmosphere–ocean ^{14}C difference. For use in mass and isotope balance calculations, one employs ^{14}C concentrations, often expressed as Δ^{14}C. This is the relative deviation of the ^{14}C concentration of a sample from that of the defined modern (and/or past) standard atmosphere, expressed in per mil.

By comparison with previous related studies (Campin et al., 1999), our empirical data set is much enlarged and more robust. Moreover, it stays below the fairly complex "pipeline" system characteristic of intermediate-water circulation (Burke and Robinson, 2012), hence promises an improved understanding of the glacial-to-deglacial changes in the carbon inventory of the abyssal ocean.

The spatial distribution of modern apparent ^{14}C ventilation ages (in our study abbreviated as "ventilation ages" and/or "Δ^{14}C") (Matsumoto, 2007) (Fig. 1) roughly depicts
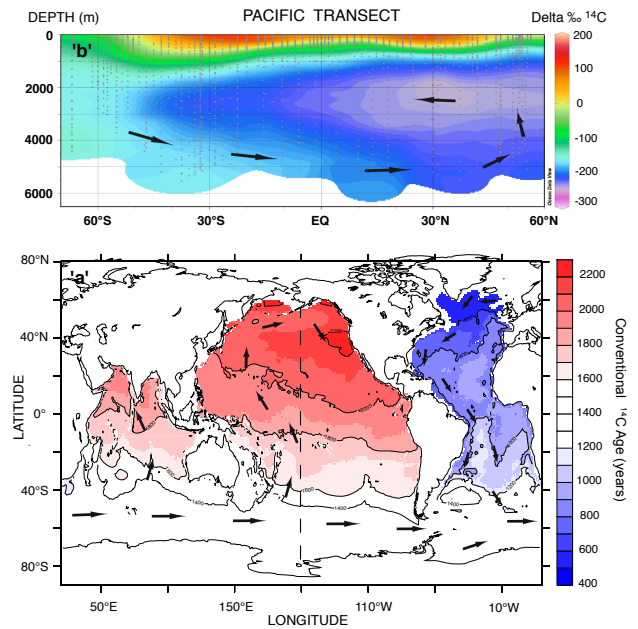

Fig. 1. Modern apparent ventilation ages based on natural radiocarbon in the ocean below 1500 m w.d. **(a)** (Matsumoto, 2007, modified; copyright granted by J. Wiley and Sons.) Arrows indicate long-term directions of circulation. Broken line = transect position. **(b)** North–South transect across the Pacific at 160° W (based on GLODAP data; Key et al., 2004).

the sources and centennial-scale directions in the circulation of the abyssal ocean, that is the basis for the concept of an "ocean salinity conveyor belt" which starts from the northern North Atlantic and terminates in the North Pacific after almost 2000 ^{14}C yr (Stommel, 1961; Broecker, 1991). Accordingly, past changes in the ventilation age of the abyssal ocean enable us to draw preliminary conclusions regarding deglacial changes in the source, intensity, and global directions of ocean MOC (Rahmstorf, 2006), changes to be reconciled with independent evidence from other proxies such as benthic δ^{13}C (McCave et al., 2008; Sarnthein et al., 1994), Pa/Th (Negre et al., 2010), and Nd records (Basak et al., 2010).

Our approach to reconstructing past oceanographic conditions rests essentially on the largely linear relationship between modern ventilation ages, or rather Δ^{14}C, and modern concentrations of dissolved inorganic carbon (DIC) in the deep ocean below > 2000 m w.d. (GLODAP data; Key et al., 2004), as shown in Sect. 2.1 and Fig. 2a. Our working hypothesis is that this relation may be used to estimate carbon storage in the deep ocean during the LGM and the deglacial. Section 2 is largely devoted to a discussion of whether this hypothesis is tenable. Having constrained the uncertainty range of the DIC–Δ^{14}C relation (Fig. 2b), extrapolation enables us in Sect. 4 to estimate tentatively the scope of the glacial-to-deglacial redistribution of carbon inventories on
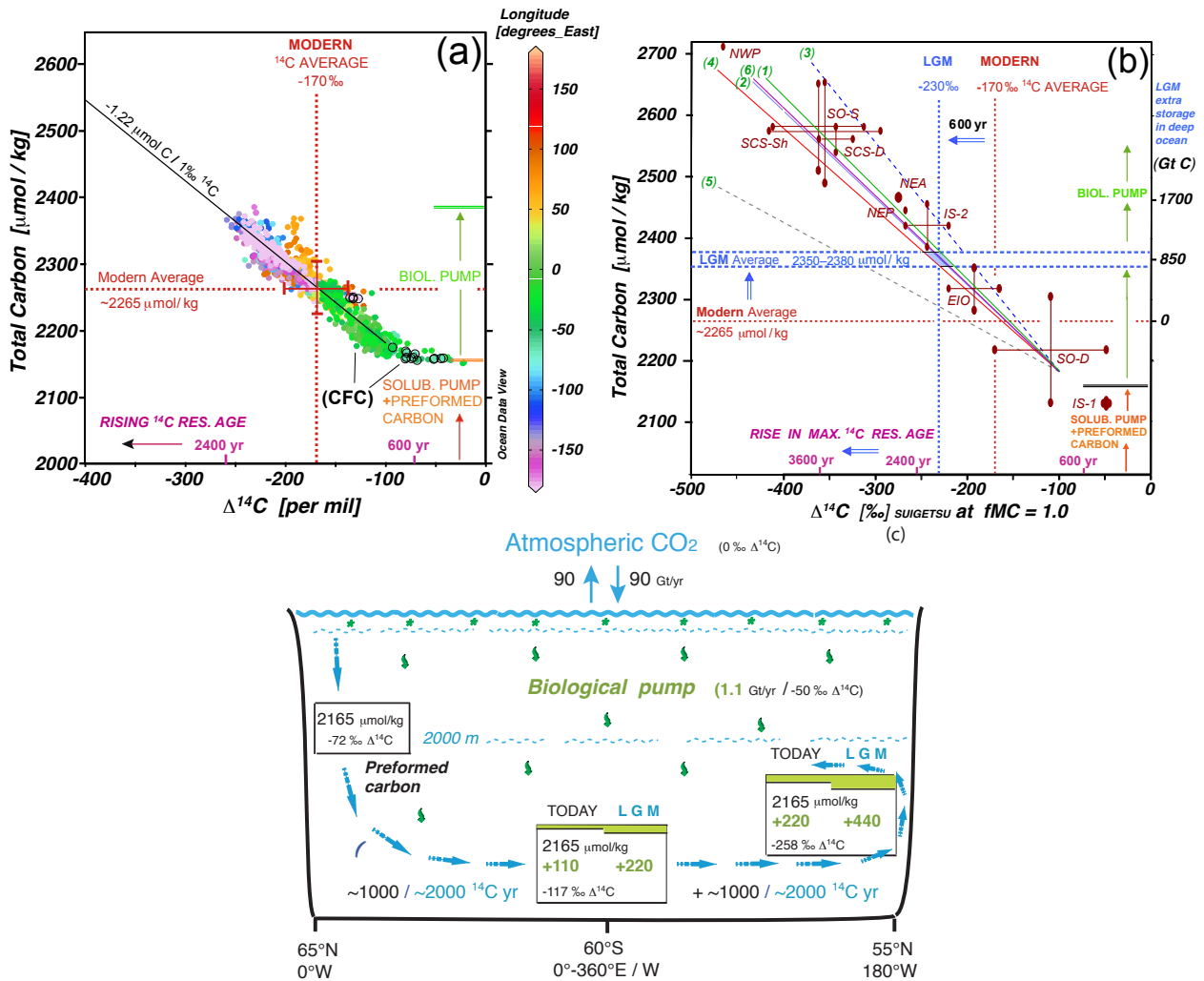
Fig. 2. (a) Ratio of total dissolved inorganic carbon (DIC) per kg vs. benthic Δ^{14}_{paleo}C and ^{14}C ventilation age for fMC = 1 of ocean waters below > 2000 m w.d. **(a)** Modern, volumetrically unweighted GLODAP data (Key et al., 2004) for longitudes of the Atlantic (green), the western (orange) and eastern Indian Ocean and Pacific (pink and blue). Standard deviation is ±32.8 ‰ for Δ^{14}C and ±40.2 µmol kg^{-1} for DIC. Black open circles mark deep waters with chlorofluorocarbon (CFC) concentrations > 0.1 pmol kg^{-1} as tracers of modern anthropogenic influence in the northern North Atlantic and Weddell Sea Bottom Water (orange dots). Modern ventilation ages of 600 to 2400 ^{14}C yr average at 1500 ^{14}C yr = −170 ‰ Δ^{14}C. **(b)** LGM regional estimates and LGM variability ranges of DIC–Δ^{14}C and age ratio (red oval dots) constrained for several key ocean regions: EIO = Eastern Indian Ocean; IS-1 = Icelandic Sea Mode 1; IS-2 = Icelandic Sea Mode 2; NEA = Northeast Atlantic; NEP = Northeast Pacific; NWP = Northwest Pacific; SCS-S = shallow South China Sea; SCS-D = deep South China Sea; SO-D = deep Southern Ocean; SO-S = shallow Southern Ocean. Estimates were calculated using the assumption of stable regional regression slopes. Green numbers at upper left refer to sea regions defined in Fig. 3. Regression slopes are −1.49 µmol kg^{-1}/Δ^{14}C (1), −1.43 µmol kg^{-1}/Δ^{14}C (2), −1.87 µmol kg^{-1}/Δ^{14}C (3), −1.27 µmol kg^{-1}/Δ^{14}C (4), −0.79 µmol kg^{-1}/Δ^{14}C (5), and −1.44 µmol kg^{-1}/Δ^{14}C (6). Following **(a)**, Δ^{14}C values for intra-LGM age differences between atmosphere and deep-water (= apparent benthic ventilation ages) and related DIC values are calculated for "paleo" fMC = 1 (Table 1). LGM ventilation ages show average end members of < 500 Δ^{14}C yr in the Icelandic Sea, ∼ 3600 ^{14}C yr in the Southern Ocean, and 5000 ^{14}C yr in the Northwest Pacific, and result in an overall conservative arithmetic mean of 2100 ^{14}C yr equal to −230 ‰ of fMC (fraction of Modern Carbon). Blue values (µmol kg^{-1}) show mean DIC content of the deep ocean, estimated for a mean LGM ventilation age of 2100 ^{14}C yr. Gt C scale at upper right labels total DIC mass in the LGM ocean, stored in addition to the modern 38 100 Gt DIC, with 1 µmol DIC kg^{-1} corresponding to 8.5 Gt C in the total ocean at > 2000 m w.d. (deep-sea morphology of Amante and Eakins, 2009). Biol. Pump = "Biological Pump", Solub. Pump = "Solubility Pump". Blue arrows display Holocene-to-LGM shifts. **(c)** Scheme of the carbon inventory of ocean deep water for modern and LGM times. The ^{14}C ages and carbon contents are subject to a delicate balance between (1) the gradual aging of preformed carbon from the northern North Atlantic (black DIC values) up to the subpolar North Pacific and (2) the incremental absorption of young biogenic organic and inorganic carbon (green DIC values) supplied by the biological pump from the sea surface. During the LGM the average transit time (blue age values) was prolonged, hence the global effect of the biological pump possibly doubled.

the basis of observed coeval shifts in the average ventilation age of deep waters. In particular, we test the LGM scenario and compare it with that of HS-1 and the warm Bølling–Allerød (B/A) interstadial. In Sect. 4.3 we check the credibility of the predicted shifts in the DIC concentration of the abyssal ocean by comparison with patterns deduced from other proxies such as B/Ca records (Yu et al., 2010). Finally, Sect. 4.4 shows that the deglacial venting of the deep ocean results in a transfer of carbon to the atmosphere via the dynamic ocean–atmosphere exchange. This process would provide both the amount of carbon and the ^{14}C concentration for the early deglacial drop in atmospheric Δ^{14}C by 190 ± 10 ‰ over HS-1 (Broecker and Barker, 2007).

2 Present and past linkages between ^{14}C ventilation ages, dissolved carbon, and nutrients in the abyssal ocean

2.1 Spatial distribution of modern ^{14}C ventilation ages

Today, the spatial distribution of apparent ^{14}C ventilation ages (Matsumoto, 2007) reveals a gradual aging of ocean deep waters, which documents the long-term thermohaline circulation pattern of the "global salinity conveyor belt", starting from downwelling sites in the northern North Atlantic and ending with a gradual upward diffusion in the upper deepwater of the northern Indian and North Pacific oceans (Fig. 1a, b). Bottom-up admixture of rejuvenated Antarctic Bottom Water (AABW), formed in the Weddell and Ross seas, results in Indo-Pacific deep-water ages a little lower than the actual ^{14}C ventilation age of the main (North Atlantic) deep-water mass would have been since its last contact with the atmosphere, as shown by Campin et al. (1999) for the Pacific.

Today the oldest waters are not found in the deepest basins of the Pacific, which are relatively small, but rather in the more extended volume of upper deep waters at 2000–3000 m depth. Since the basic mechanisms driving deep-water formation and ocean circulation must have been the same, we assume this pattern also applied to the LGM and deglacial. Indeed, we have found first support for this assumption in our LGM data sets; moreover, in our HS-1 data as far as the northeast Atlantic is concerned (Table 1).

Different from Matsumoto (2007), we employ for all figures that display modern DIC, potential alkalinity, and oxygen, the complete ungridded, non-interpolated Δ^{14}C data set of GLODAP at > 2000 m w.d. The interpolation/extrapolation method employed by Matsumoto (2007) has been explained in detail by Key et al. (2004). We do not discuss details, since potential interpolation errors linked to Matsumoto's approach do not apply to our study. Notably, we relate quantities such as DIC, potential alkalinity (that is the sum of total alkalinity and nitrate; abbreviated POTALK), nutrients, and oxygen to ventilation age rather than to vol-

ume. Thereby we avoid potential problems arising from a patchy spatial distribution of data. In contrast to the database used for Figs. 2a and 3–6, we do employ the interpolated modern deep-water ventilation age shown in the gridded data map of Matsumoto (2007) to derive the age anomalies between LGM, HS-1, B/A, and today for each core site listed in Table 1 by means of simple comparison with the reconstructed ventilation age estimate.

2.2 Solubility pump and preformed carbon: present

The deep-ocean carbon reservoir is fed by the "solubility pump" plus "preformed" carbon, initially dissolved and downwelled by juvenile deep waters from the ocean surface and atmosphere (Raven and Falkowski, 1999; Sigman et al., 2010). Later additional carbon is added to the deep ocean by the "biological pump", which is the export flux of particulate organic and inorganic biogenic carbon from the surface ocean (Schlitzer, 2002). Figure 2a shows the relationship between DIC and Δ^{14}C, that starts with an initial concentration of ~ 2165 µmol DIC kg^{-1} sea water at -72 ‰ Δ^{14}C in the source region of North Atlantic Deepwater (NADW). The significance of the single data points is discussed in Supplement #1. The initial DIC content represents the amount of preformed carbon plus solubility pump, which is ten times larger than the total contribution of the biological pump and clearly dominates the abyssal carbon inventory. By contrast, the biological pump leads to a gradual, almost linear rise in DIC, finally summing up to ~ 220 µmol DIC kg^{-1} over a time span of 1800 ^{14}C yr with increasing distance from the source of NADW. The regression slope of DIC vs. Δ^{14}C is controlled by a delicate balance between the gradual aging of preformed carbon and an ongoing input of young carbon the biological pump supplies from the sea surface (scheme in Fig. 2c).

Towards the minimum ventilation age of 400–600 ^{14}C yr (Fig. 2a), the regression of dissolved carbon vs. ventilation age extends into a long "horizontal tail" of less negative Δ^{14}C values. This tail is located in the North Atlantic, right on the downwelling branch of NADW, at sites where the exchange of carbon between atmosphere and deep ocean is particularly fast. Moreover, a closer look at the regression also reveals a small but distinct "bump", that is a small number of positive outliers in the DIC–Δ^{14}C plot, which deviate from the general regression slope near -135 ‰ Δ^{14}C by 30 ‰ Δ^{14}C. These anomalies facilitate our understanding of (1) the processes that control the gradual increase in apparent ^{14}C ventilation ages and (2) the potential to extrapolate the Δ^{14}C–DIC relationship of Fig. 2 to climatic scenarios in the past. Both anomalies in Δ^{14}C are marked by enhanced concentrations of chlorofluorocarbons (CFC11, produced post-1950; > 0.1 pmol kg^{-1} sea water) that clearly trace the modern anthropogenic influence, thus marking an increased uptake of anthropogenic carbon including bomb ^{14}C, which needs to be ignored in our discussion. The bump in the

Table 1a. Variability range of shifts in ^{14}C ventilation age of deep waters vs. today (Matsumoto, 2007) and related shifts in DIC (Fig. 2a), alkalinity (Fig. 4), and CO_3^{2-} (in μmol kg^{-1}) deduced for the LGM, HS-1, and B/A and various ocean regions below 1500–2000 m w.d. Δ^{14}C values (‰) for intra-LGM, intra-HS-1, and intra-B/A age differences between atmosphere and deep-water (calculated from apparent benthic ventilation ages; yr) and related DIC, alkalinity, oxygen, and PO$_4$ estimates (Figs. 2, 4, 6), moreover the difference between these Δ^{14}C values and their modern correlatives are all calculated for a fraction of "paleo" Modern Carbon (fMC) = 1.0. Using the modern regression slopes characteristic of different regions (based on GLODAP data; Key et al., 2004), we also list average maximum O$_2$ concentrations and the ratio of PO$_4$ vs. ventilation age. Records PS2644 and RAPiD-10-1P are incorporated from above 1500 m w.d., as these sites match immediate source regions of modern NADW to the north and south of Iceland, except for HS-1, where they record a northward flow of intermediate waters (Fig. 3b). From less than 2000 m w.d. we incorporate records of Site 17 940 from 1727 m in the South China Sea, since it is bathed in deep waters entrained from Upper Pacific Deepwater, and Site MD01-2378 from 1787 m depth in the Eastern Indian Ocean, which is bathed in Upper Indian Ocean Deepwater. Because of too low benthic specimen numbers in Core PS2644, the B/A age for the Icelandic Sea is not based on direct dating but on analogies to today, deduced from high local benthic δ^{13}C values of 1.1–1.4 ‰ (Voelker, 1999), thus earmarked by a question mark in Fig. 3a.

Ventilation age (yr)	Ventilation age (‰Δ^{14}C)	DIC (μmol kg^{-1})	Potential alkalinity (μmol kg^{-1})	CO_3^{2-} (μmol kg^{-1})	Max. O$_2$ (μmol kg^{-1})	PO$_4$ (μmol kg^{-1})
Icelandic Sea[a]						
MODERN VALUES						
550	−66	ave. DIC = 2204	ave. POTALK = 2368	ave. CO_3^{2-} = 100–105	ave. O$_2$ = 241	ave. PO$_4$ = 1.58
		ΔDIC = −1.49·Δ^{14}C	ΔPOTALK = −1.15·Δ^{14}C	ΔCO_3 = ΔPOTALK-ΔDIC	ΔO$_2$ = 0.71·Δ^{14}C	ΔPO$_4$ = -0.01·Δ^{14}C
PAST SHIFTS						
LGM:*						
+1450–+2100	−165–−230	+246–+343	+190–+264	−56–−79	124–78	+1.65–+2.30
−180–−110	+23–+14	−34–−21	−26–−16	+8–+5	257–251	−0.14–−0.23
HS-1:*						
+700–+1400	−83–−160	+123–+238	+95–+184	−28–−54	182–127	+0.83–+1.6
B/A:						
±0	±0	±0	±0	±0	241	±0
Northeastern North Atlantic[b]						
MODERN VALUES						
600	−72	ave. DIC = 2204	ave. POTALK = 2368	ave. CO_3^{2-} = 100–105	ave. O$_2$ = 241	ave. PO$_4$ = 1.58
		ΔDIC = −1.49·Δ^{14}C	ΔPOTALK = −1.15·Δ^{14}C	ΔCO_3 = ΔPOTALK-ΔDIC	ΔO$_2$ = 0.71·Δ^{14}C	ΔPO$_4$ = -0.01·Δ^{14}C
PAST SHIFTS						
LGM:						
+1800–+2000	−201–−220	+300–+317	+231–+253	−69–−64	98–85	+2.01–+2.20
HS-1:*						
+4000–+4500	−392–−429	+584–+639	+451–+493	−133–−146	0	+3.92–+4.29
B/A:						
0–−1000	±0–+117	±0–−174	±0–−135	±0–+39	241–158	±0–−1.17
Western North Atlantic[c]						
MODERN VALUES						
700	−83.5	ave. DIC = 2204	ave. POTALK = 2368	ave. CO_3^{2-} = 100–105	ave. O$_2$ = 241	ave. PO$_4$ = 1.58
		ΔDIC = −1.49·Δ^{14}C	ΔPOTALK = −1.15·Δ^{14}C	ΔCO_3 = ΔPOTALK-ΔDIC	ΔO$_2$ = 0.71·Δ^{14}C	ΔPO$_4$ = −0.01·Δ^{14}C
PAST SHIFTS						
HS-1:						
+500–+1700	−60–−191	+89–+285	+69–+220	−20–−65	198–105	+0.60–+1.91
Southern Ocean (Atlantic sector)[d]						
MODERN VALUES						
1200	−140	ave. DIC = 2248	ave. POTALK = 2409	ave. CO_3^{2-} = 80	ave. O$_2$ = 226	ave. PO$_4$ = 2.14
		ΔDIC = −1.43·Δ^{14}C	ΔPOTALK = −1.06·Δ^{14}C	ΔCO_3 = ΔPOTALK-ΔDIC	ΔO$_2$ = 1.26·Δ^{14}C	ΔPO$_4$ = −0.02·Δ^{14}C
PAST SHIFTS						
at 3700 m water depth:						
LGM:						
+1600–+3100	−181–−320	+259–+458	+192–+339	−67–−119	0	+3.62–+6.4
HS-1:						
+700–+2400	−83–−258	+119–+369	+88–+273	−31–−96	121–0	+1.66–+5.16
B/A:						
−300–+1000	+37–−117	−53–+167	−39–+124	+14–−43	273–79	−0.74–+2.34
at 5000 m water depth:						
LGM:						
−800–+300	+92–−36	−132–+51	−98–+38	+34–−13	341–181	−1.84–+0.72
HS-1:						
+1050–+600	−122–−70	+174–+100	+129–+74	−45–−26	72–138	+2.44–+1.40
B/A:						
+1100–−100	−130–+12	+186–−17	+138–−13	−48–+4	62–241	+2.60–−0.24
Southern Ocean (Pacific sector)						
MODERN VALUES						
1400–1600	−160–−181	ave. DIC = 2272	ave. POTALK = 2424	ave. CO_3^{2-} = 79	ave. O$_2$ = 193	ave. PO$_4$ = 2.28
		ΔDIC = -0.79·Δ^{14}C	ΔPOTALK = −0.83·Δ^{14}C	ΔCO_3 = ΔPOTALK-ΔDIC	ΔO$_2$ = 1.13·Δ^{14}C	ΔPO$_4$ = −0.0048·Δ^{14}C

* End members of oscillating deepwater regimes.

Table 1a. Continued.

Ventilation age (yr)	Ventilation age (‰ Δ^{14}C)	DIC (µmol kg^{-1})	Potential alkalinity (µmol kg^{-1})	CO$_3^{2-}$ (µmol kg^{-1})	Max. O$_2$ (µmol kg^{-1})	PO$_4$ (µmol kg^{-1})
Eastern Indian Ocean[e]						
MODERN VALUES						
1950	−215	ave. DIC = 2291	ave. POTALK = 2457	ave. CO$_3^{2-}$ = 84	ave. O$_2$ = 174	ave. PO$_4$ = 2.34
		ΔDIC = −1.27·Δ^{14}C	ΔPOTALK = −1.18·Δ^{14}C	ΔCO$_3$ = ΔPOTALK-ΔDIC	ΔO$_2$ = 1.7·Δ^{14}C	ΔPO$_4$ = -0.0075·Δ^{14}C
PAST SHIFTS						
LGM:						
+50−−500	−6−+64	+8−−81	+7−−76	−1−+5	164−283	+0.05−−0.48
HS-1:						
−200−−100	+25−+13	−32−−17	−30−−15	+2	216−196	−0.18−−0.10
B/A:						
−300−−500	+ 37−+64	−47−−81	−44−−76	+3−+5	237−283	−0.28−−0.48
South China Sea[f]						
MODERN VALUES						
1900	−210	ave. DIC = 2328	ave. POTALK = 2477	ave. CO$_3^{2-}$ = 73	ave. O$_2$ = 141	ave. PO$_4$ = 2.55
		ΔDIC = −1.44·Δ^{14}C	ΔPOTALK = −0.96·Δ^{14}C	ΔCO$_3$ = ΔPOTALK-ΔDIC	ΔO$_2$ = 1.68·Δ^{14}C	ΔPO$_4$ = −0.009·Δ^{14}C
PAST SHIFTS						
at 1727 m water depth:						
LGM:						
+1100−+2350	−130−−254	+187−+366	+125−+244	−62−−122	0	+1.17−+2.29
HS-1:						
−550−−1500	+71−+205	−102−−295	−68−−197	+34−+98	260−485	−0.64−−1.85
B/A:						
−1100−−400	+130−+50	−187−−72	−125−−48	+62−+24	360−225	−1.17−−0.45
at 2700 m water depth:						
LGM:						
+1250−+1700	−144−−191	+207−+275	+138−+183	−69−−92	0	+1.30−+1.72
HS-1:						
+800−+1450	−95−−165	+137−+238	+91−+158	−46−−80	0	+0.86−+1.49
B/A:						
±0	±0	±0	±0	±0	141	±0
Northwest Pacific Ocean[g]						
MODERN VALUES						
2100	−230	ave. DIC = 2328	ave. POTALK = 2477	ave. CO$_3^{2-}$ = 73	ave. O$_2$ = 141	ave. PO$_4$ = 2.55
		ΔDIC = −1.44·Δ^{14}C	ΔPOTALK = −0.96·Δ^{14}C	ΔCO$_3$ = ΔPOTALK-ΔDIC	ΔO$_2$ = 1.68·Δ^{14}C	ΔPO$_4$ = -0.009·Δ^{14}C
PAST SHIFTS						
LGM:						
+2740	−289	+416	+277	−139	0	+2.60
HS-1:						
+1900−+900	−211−−106	+304−+153	+203−+102	−101−−51	0	+1.90−+ 0.95
B/A:						
+500−−500	−60−+60	+86−−86	+58−−58	−28−+28	40−242	+0.54−−0.54
Northeast Pacific Ocean[h]						
MODERN VALUES						
2200	−240	ave. DIC = 2328	ave. POTALK = 2477	ave. CO$_3^{2-}$ = 73	ave. O$_2$ = 141	ave. PO$_4$ = 2.55
		ΔDIC = −1.44·Δ^{14}C	ΔPOTALK = −0.96·Δ^{14}C	ΔCO$_3$ = ΔPOTALK-ΔDIC	ΔO$_2$ = 1.68·Δ^{14}C	ΔPO$_4$ = −0.009·Δ^{14}C
PAST SHIFTS						
LGM:						
+300	−37	+53	+36	−17	79	+0.33
HS-1:						
−1150−+300	+154−−37	−222−+53	−148−+36	+74−−17	400−79	−1.39−+0.33
B/A:						
+200−−750	−25−+98	+36−−141	+24−−94	−12−+47	99−306	+0.23−−0.88

Table 1b. List of core locations (compare Fig. 7) and techniques #1–5 used to obtain benthic ventilation ages and shortly explained in the Methods Section 3, as well as published data sources. Ventilation ages derived by technique #5 (Fig. S1) were generated on the basis of ^{14}C plateau boundary ages identified in the new 'Suigetsu' atmospheric Δ^{14}C record (Bronk Ramsey et al., 2012). Apparent ventilation ages and data sources listed in Table 1 and Fig. 7 are deposited in the PANGAEA databank (http://www.pangaea.de/PangaVista)

	CORE NUMBER	LOCATION	published by	ABSOLUTE CHRONOLOGY deduced by
a	PS2644	67°52′ N, 21°46′ W, 777 m w.d.	(Sarnthein et al., 2007; Suppl. Fig. S1a)	Technique # 5
b	RAPiD-10-1P	62°59′ N, 17°35′ W, 1237 m w.d.	(Thornalley et al., 2011)	Technique # 3 plus # 4
	RAPiD-15-4P	62°18′ N, 17°08′ W, 2133 m w.d.	(Thornalley et al., 2011)	
	RAPiD-17-5P	61°29′ N, 19°32′ W, 2303 m w.d.	(Thornalley et al., 2011)	
	MD99-2334	37°48′ N, 10°10′ W, 3146 m w.d.	(Skinner et al., 2010)	
c	Coral transects	33°30–39°0′ N, 60°30–62°30′ W, 1700–2300 m w.d.	(Robinson et al., 2005)	Technique # 1
d	TNO57-21	41°06′ S, 7°48′ E, 4981 m w.d.	(Barker et al., 2010)	Technique # 2
	MD07 3076	44°05′ S, 14°13′ E, 3770 m w.d.	(Skinner et al., 2010)	Technique # 4
e	MD01-2378	13°05′ S, 123° 43.3′ E, 1783 m w.d.	(Sarnthein et al., 2011; Suppl. Fig. S1e)	Technique # 5
f	GIK 17940	20°07′ N, 117°23′ E, 1727 m w.d.	(Sarnthein et al., 2007; Suppl. Fig. S1f$_1$)	Technique # 5
	SO50-37	18°55′ N, 115°45′ E, 2695 m w.d.	(Broecker et al., 1990; adapted by Sarnthein et al., 2007; Suppl. Fig. S1f$_2$)	Technique # 5
	(records of Pacific inflow waters entraining upper Pacific deep waters)			
g	MD01-2416	51°27′ N, 167°73′ E, 2317 m w.d.	(Sarnthein et al., 2007; Suppl. Fig. S1g$_1$)	Technique # 5
	MD98-2181	6°18′ N, 125°49′ E, 2114 m w.d.	(Broecker et al., 2004; plus Suppl. data Fig. S1g$_2$)	Single Δ^{14}C estimate based on synsedimentary wood chunks and planktic foraminifera (equivalent of 2550 yr for HS-1)
h	MD02-2489	54°39′ N, 148°92′ W, 3640 m w.d.	(Gebhardt et al., 2008; Suppl. Fig. S1h)	Technique # 5 Techniques #1 to 5 described in Sect. 3

regression slope near −135 ‰ Δ^{14}C is confined to a narrow longitudinal range between ∼ 20° W and 30° E in the South Atlantic, precisely the region where modern Weddell Sea Bottom Water (WSBW) mixes with NADW and Circumpolar Water (CPW) in the Southern Ocean (Matsumoto, 2007). The admixed WSBW conveys additional ^{14}C from a more recent, though weak, contact with the atmosphere, thus having lower ^{14}C ventilation ages than the NADW after > 700 ^{14}C yr of circulation. Accordingly, the admixture results in a slight rejuvenation of CPW and an increased level of preformed carbon. This additional carbon marks these waters continuously as long as they flow farther east into the Indo-Pacific, hence inducing a slight upward shift of the fairly robust regression slope in Fig. 2a. A further source of ^{14}C may be located in the Ross Sea, 170–180° E. However, CFC data from this region (Orsi et al., 2002) indicate an only marginal contribution of anthropogenically affected, hence very young CO_2, which we regard as negligible. Supplement #2 discusses a lack of DIC depletion in surface waters only shortly exposed to the atmosphere.

2.3 Solubility pump and preformed carbon: past

Our working hypothesis is that the present DIC–Δ^{14}C relationship can be used to estimate the storage capacity of DIC in the LGM abyssal ocean. Thus, we first roughly assess past changes in the minimum level of the "solubility pump plus preformed carbon", today contributing 2165 µmol DIC kg^{-1} at the main regions of peak glacial deep-water formation in the North Atlantic Ocean and the Labrador and Norwegian seas. Our estimates consider the joint effect of a peak-glacial drop in atmospheric CO_2 of 30 % (Monnin et al., 2001), a 3 °C drop in glacial SST (based on census counts of planktic foraminifera; Pflaumann et al., 2003), a contemporaneous 1 psu rise in sea surface salinity (based on census counts and δ^{18}O records of planktic foraminifera; Duplessy et al., 1991a), and a slightly elevated alkalinity (+3 %; as the result of increased salinity and enhanced cation concentrations due to lowered sea level), following widely accepted LGM proxy data such as benthic δ^{13}C transects (Sarnthein et al., 1994). Counterintuitively, the outlined variations in boundary

conditions induce little change, hardly exceeding 3 per mil of the carbon concentration ascribed to preformed DIC, which constitutes ca. 90 % of total DIC in the deep ocean. Changes in glacial DIC were thus largely associated with the biological pump.

2.4 Transfer functions present to past: caveats and solutions

To establish transfer functions for deducing past concentrations of DIC, alkalinity, oxygen, and PO$_4$ in the deep ocean from measured Δ^{14}C concentrations (used as a proxy of ^{14}C ventilation age), modern ventilation ages of deep waters are compared with modern concentrations of DIC, alkalinity, O$_2$, and PO$_4$ in the abyssal ocean below 2000 m w.d. (GLODAP data; Key et al., 2004; Table 1). In our text we only refer to stoichiometric principles as far as they concern the gradients of our age–organic-carbon derived DIC, age–alkalinity, age–oxygen, age–PO$_4$, and age–CO$_3^{2-}$ relationships. We use the slopes of organic carbon (derived from potential alkalinity) vs. age and oxygen vs. age to calculate the organic carbon (C$_{org}$) / oxygen ratio of respiration, which gives a simple check of consistency (for mol ratios see Supplement #3).

Modern ^{14}C ventilation ages increase from about 600 up to 2400 ^{14}C yr with increasing distance from the deep-water source (Fig. 2a). This aging of deep waters by 1800 ^{14}C yr matches an increase of 230 µmol DIC kg^{-1} at the terminus of the conveyor belt in the Pacific, on average 1.22 µmol DIC kg^{-1} per 1 ‰ decrease in Δ^{14}C. In view of the deep-ocean volume > 2000 m w.d. considered here, which represents ∼ 50 % of the total ocean, an average concentration of 1 µmol DIC kg^{-1} corresponds to 8.5 Gt C (based on ETOPO-60; Amante and Eakins, 2009, and GLODAP data). Hence the regression slope of Fig. 2a implies that the modern abyssal ocean is receiving ∼ 1.1 Gt C per ^{14}C yr deep-water transit time (Fig. 2c). As shown below, we assign this carbon uptake to the "biological pump". It incorporates 0.64 Gt C/^{14}C yr mostly from remineralized particulate organic matter (POC) plus 0.45 Gt C/^{14}C yr from the dissolution of calcium carbonate (PIC). In total, the organic carbon flux below 2000 m depth amounts to no more than ∼ 6 % of the export flux from the surface ocean (Schlitzer, 2002), thus coming close to independent estimates based on sediment traps (Antia et al., 2001). Likewise, our estimates of the biological pump agree with flux data of PIC that amount to 0.6 Gt C yr^{-1}, > 0.1 Gt C yr^{-1} of which are buried in the sediment (Berelson et al., 2007), hence delivering > 0.45 Gt yr^{-1} to deep waters (also see Supplement #4).

The outlined gross fluxes of POC and PIC, possibly in combination with a slower but prolonged remineralization of POC, may have varied over the past due to changes in both the NO$_3$ of surface waters and the "rain ratio" between organic and carbonate carbon (Berger and Keir, 1984), leaving an imprint on the alkalinity of deep waters. This may prevent a simple extrapolation of the modern average DIC age ratio
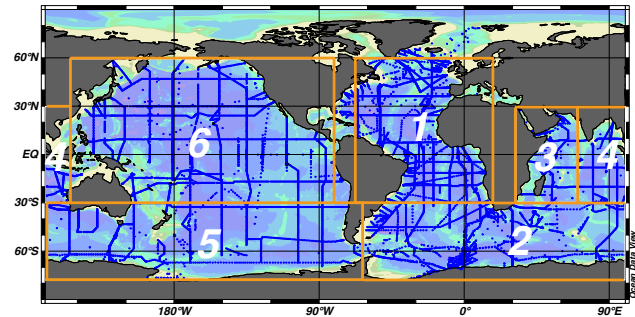

Fig. 3. Six major ocean regions used for testing the uncertainty range of the relationships of DIC and total alkalinity vs. Δ^{14}C (at > 2000 m w.d.). To the north, Region 3 ends in a monsoon-driven belt of high upwelling productivity off Somalia and southern Arabia. Region 5 includes the low-nutrient subtropical and subpolar southern Pacific ocean.

of −1.22 µmol kg^{-1} per ‰ Δ^{14}C to past climatic scenarios. Although we cannot derive for the glacial ocean any DIC age relationship for lack of data, we may use for its estimation a probability argument that is based on the variability of the DIC age relationship over six major basins in the modern ocean (Fig. 3).

Modern Δ^{14}C distributions show regression slopes of the four largest ocean basins, which only range from −1.27 to −1.49 µmol DIC kg^{-1} per ‰ Δ^{14}C (Figs. 2b and 3). Thus, most slopes are closely comparable, despite different water mass conversion and circulation conditions in the different basins they represent. Moreover, published evidence (Sarnthein et al., 1994; Curry and Oppo, 2005; McCave et al., 2008) indicates a glacial deep-water circulation in the North Atlantic and Southern oceans that did not differ very much from the Holocene. Hence the LGM overall thermohaline overturning circulation worked in a way similar to today, although AABW had likely expanded in the bottommost ocean during glacial times.

Only two ocean regions (nos. 3 and 5 in Fig. 3) deviate from the general homogeneity of regression slopes. One is the far northwestern Indian Ocean, showing a steep slope of −1.87 µmol DIC kg^{-1} per ‰ Δ^{14}C. This basin is controlled by high carbon fluxes due to strong upwelling productivity in the Arabian Sea, and hence is an unlikely analog for the glacial ocean at large, and hence is ignored. In contrast, a much lower ratio of −0.79 µmol kg^{-1} per ‰ Δ^{14}C is currently characteristic of Region 5 in the southern South Pacific (Fig. 3), and might be an analog for some glacial and deglacial basins. East of Australia the modern ocean shows a major eastward decrease in the (dust-borne) nutrient supply. Thus, both carbon flux and the PO$_4$–age ratio are four times lower in the Pacific sector than in the Atlantic and Indian sectors of the modern Southern Ocean (Table 1). Yet this decrease did not necessarily apply to the LGM, when enlarged Patagonian and Australian deserts in combination
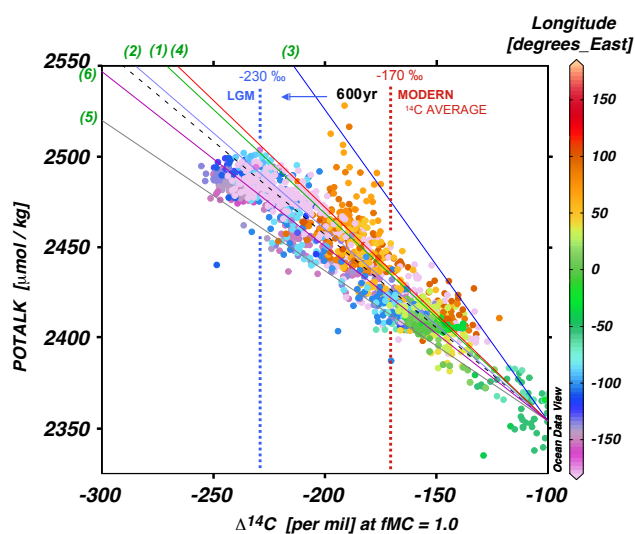
Fig. 4. Potential alkalinity (POTALK) vs. Δ^{14}C in modern ocean waters below 2000 m w.d., based on volumetrically unweighted GLODAP data (Key et al., 2004), showing the differential influence of deep-ocean calcite dissolution on total alkalinity in six major ocean regions (green numbers at upper left) as delineated in Fig. 3. Regression slopes are -1.15 (1), -1.06 (2), -1.71 (3), -1.18 (4), -0.83 (5), and -0.96 µmol kg^{-1} per ‰ Δ^{14}C (6). Global average regression line (-1.03 µmol kg^{-1} per ‰ Δ^{14}C) is hatched. Color scale indicates eastern longitudes of deep waters. Vertical dotted lines mark modern and LGM average ventilation ages of 1500/2100 ^{14}C yr.

with increased storminess led to a significant rise in the flux of dust and iron to the southern South Pacific. In particular, this rise applies to a broad belt between 20° and 50–60° S (Thiede, 1979), as recently confirmed by records of cores E33-22, E11-2, E14-6, and E20-10 (Chase et al., 2003). However, the increased dust flux did not apply to sites further south and west, such as to the region south of Tasmania at 55–65° S. Thus we may assume that the glacial-to-deglacial productivity in South Pacific Region 5, to the north of ∼ 60° S, was largely similar to that of Region 2 further west, but possibly somewhat reduced to the south of ∼ 60° S.

In summary, the evaluation of the spatial variability of the modern DIC–Δ^{14}C relationship constrains a narrow range of gradients for different basins and conditions. Based on this and a consideration of the glacial dust input, we assume that for the whole glacial ocean the overall variability of the gradient in the DIC–age ratio hardly exceeded the modern range of -1.25 to -1.5 µmol DIC kg^{-1} per ‰ Δ^{14}C, although somewhat differently distributed. This supports our working hypothesis that the range of differential regression slopes that currently characterize sea regions 1–6 (listed in Fig. 2b and Table 1) may serve as an adequate basis for estimating DIC values for the widest possible range of scenarios of the biological pump in the modern deep ocean as well in the deep ocean of the past.

This hypothesis rests on various key assumptions that may be tested:

- On a global scale the single data points in Fig. 2a by and large comply with equal-volume units and are representative of the global ocean (data points in Fig. 3).

- The modern variability of the regression slope of DIC–Δ^{14}C incorporates the LGM range of slope variability.

- Regional slopes of DIC–Δ^{14}C are regarded as constant as long as regional nutrient fluxes remained constant.

- The LGM circulation geometry was basically similar to today, whereas deep-water transit times increased significantly. In contrast, the circulation geometry may have strongly differed during HS-1.

- In terms of the DIC–Δ^{14}C the relationship, the NADW and AABW in the Southern Ocean do not differ significantly, since AABW consists largely of "recycled" NADW.

- Global export production was widely constant (Sigman and Boyle, 2000), and thus decoupled from the transit time of ocean overturning circulation, if we assume that the global nutrient input and bulk biological pump were controlled by basically similar conditions during the LGM as today and that carbon-to-nutrient element ratios were not constant (Schneider et al., 2003). In addition, we need to reckon with a dust-borne major productivity rise in the LGM subantarctic South Pacific. This rise, however, may have been largely compensated for by a coeval productivity drop in sea ice-covered polar latitudes (Chase et al., 2003).

- Ocean intermediate waters comprise approximately the same volume as deep waters and form an integral part of the ocean carbon inventory. Its magnitude may occasionally alternate with that of deep waters.

On this basis, we employ the DIC–Δ^{14}C slope range for extrapolation to the LGM deep-water scenario, but not to intermediate waters, which are not addressed in our study. Our working hypothesis to extrapolate the modern average regression slope will need to be tested for LGM conditions by means of a general circulation model (GCM) simulation that couples changes in climate and the carbon cycle. However, all GCM runs presently available (and the output of two we have tentatively analyzed) suffer from a lack of general consensus on the properly modeled circulation geometry that applies for the LGM (Tagliabue et al., 2009) and/or from deficits in the treatment of carbon mass conservation amongst various reservoirs. In our opinion, box models are inadequate for meeting the complex and interactive scenario of the past ocean and global carbon cycle. Thus, simple two-box model calculations may demonstrate that an explanation

is physically possible, but cannot provide quantitative verification. Accordingly we regard these tests as possibly misleading, since they hardly provide robust evidence, but would stretch the paper significantly. Also, an important boundary condition for any model test, the robustness of the C : N : P element ratios resulting from organic particle remineralization (Redfield et al., 1963), appears questionable (Schneider et al., 2003). For these reasons, we constrain the present paper to our empirical data-based evidence and the working hypotheses arising from it.

3 Estimates of past deep-ocean ^{14}C ventilation ages – methods and sources

Past ^{14}C ventilation ages, like those of today, are obtained as the difference in measured ^{14}C age between contemporaneous oceanic and atmospheric samples. Oceanic samples usually consist of corals and planktic or benthic foraminifera picked from a sediment core and are easily obtained. However, securely correlated atmospheric ^{14}C samples (e.g., terrestrial plant remains) are rarely available in deep-sea sediments. Instead, the absolute age of the sampled layer is determined in marine sediment sections by means of five different techniques that provide the ^{14}C age of the contemporaneous atmosphere via radiocarbon calibration curves (Reimer et al., 2009, 2013; Bronk Ramsey et al., 2012), techniques that are shortly described below.

1. Technique #1 is based on paired U/Th- and ^{14}C-based ages of deep-water corals (as used by Adkins et al., 1998; Robinson et al., 2005; Burke and Robinson, 2012). It provides highly precise and most direct estimates of both the absolute age and the coeval ^{14}C concentration of past deep waters. To obtain ventilation ages, these ^{14}C values are compared with ("projected on") past coeval atmospheric ^{14}C concentrations displayed in the IntCal09 record (Reimer et al., 2009) using the projection method (caveats listed in Supplement #5). The accumulated LGM uncertainty of ventilation ages generally amounts to $\pm \sim 500$ yr and may rise up to $\pm \sim 1000$ yr (at 2σ). Unfortunately, samples of dated deep-water corals are limited to less than 2500 m water depth in the northwest Atlantic, and to less than 1750 m in the Drake Passage. Thus corals do trace ventilation ages of intermediate waters, but rarely of deep waters below 2000 m.

2. The ^{14}C "projection method" was frequently applied to data sets of ^{14}C ages of benthic foraminifera samples from mid- and low-latitude sites (e.g., Marchitto et al., 2007; Franke et al., 2008; Barker et al., 2010). To provide absolute age estimates, various climatic events in the sediment core were tied over inter-hemispheric distances to a mixture of age control points in the Hulu Cave speleothem δ^{18}O record and/or the annual layer-

counted time scales of Greenland and Antarctic ice core records. Yet the assumption that these climatic events were contemporaneous over inter-hemispheric distances appears by no means proven. Rather it may turn out to be spurious, since it ignores likely phase lags and leads and/or potential oceanographic see-saw effects on the order of several 100–1000 yr. This approach may be subject to severe errors as long as events with (semi-)millennial resolution and better are analyzed. Resulting LGM uncertainties may range up to $> \pm 1000$ yr. Caveats of the projection technique per se are discussed in Supplement #5.

3. In some ocean regions (e.g., North Atlantic, east of New Zealand) interbedded ash layers with radiometric age control provide fairly robust absolute age estimates that can be interpolated for dating glacial-to-deglacial planktic and benthic ^{14}C ages (to be compared with contemporaneous atmospheric ^{14}C levels). This technique requires continuous sedimentation rates, in some sediment sections difficult to check (e.g., Waelbroeck et al., 2001; Rose et al., 2010; Thornalley et al., 2011). If sedimentation rates are continuous, the composite age uncertainty of this technique ranges on centennial scales.

4. Different from low-latitude records, the absolute age control of high-latitude high-resolution marine climate records and benthic foraminifera ^{14}C ages can be promptly derived by tuning to the elaborate, in part annual-layer-based chronology of nearby ice core records. This holds true as far as significant lateral phase shifts can be excluded on the basis of logical reasoning (Thornalley et al., 2011; Skinner et al., 2010). The uncertainty of LGM and deglacial age control may range between ~ 300 and < 1000 yr.

5. The ^{14}C plateau tuning technique derives past reservoir ages of surface waters (planktic Δ^{14}C) from the difference between the average uncorrected ^{14}C age of planktic ^{14}C plateaus measured in sediment cores and the ^{14}C age of well-constrained equivalent atmospheric ^{14}C plateaus numbered 1–7 over the LGM and Termination 1 (Sarnthein et al., 2007; further details in Fig. S1; averaging techniques in Supplement #6; estimated LGM uncertainty range of ± 250–450 yr). The age-defined upper and lower boundaries of the ^{14}C plateaus provide absolute age estimates that have been defined at ^{14}C plateaus of the varve-counted atmospheric ^{14}C record of Lake Suigetsu. The sum of planktic ^{14}C ventilation age plus the difference between paired raw benthic and planktic ^{14}C ages provide deep-ocean ventilation ages (benthic Δ^{14}C; Fig. S1). This technique requires sediment cores with sedimentation rates exceeding 6–10 cm kyr^{-1}.

The five outlined reconstruction techniques all produce ^{14}C ventilation ages that differ significantly from estimates derived from a simple addition of benthic–planktic age differences to planktic ^{14}C reservoir ages that are presumed to be constant, or, to deviate only a little from a modern average of 400–550 yr, an assumption indefensible today (Stuiver and Braziunas, 1993; Reimer et al., 2009). In most cases, the latter estimates will result in deep-water ventilation ages that are far too low and, in turn, provide calendar age estimates possibly exceeding the actual age by up to 2000 yr. Thus we exclude such ages from the data set of this study. Various lines of evidence supporting the temporarily high planktic reservoir ages that emerge from dating techniques 1–5 are summarized in Supplement #7.

For age calibration we use the varve-counted atmospheric ^{14}C record of Lake Suigetsu (Bronk Ramsey et al., 2012) for several reasons.

- The ^{14}C record of Lake Suigetsu sediments, continuously varved beyond ∼ 10 cal. ka, is the only decadal-to-centennial scale resolution, purely atmospheric ^{14}C and Δ^{14}C record available beyond 13.9 cal. ka (Reimer et al., 2013).

- Reworking of fossil plant materials selected for ^{14}C dating affects neither the varve-based nor the model-based calibrated time scales. Moreover, its influence was constrained by selecting fragile plant materials that cannot survive reworking.

- For the peak glacial and the deglacial we consider the varve-counted time scale superior to the modeled Suigetsu time scale. The latter is tuned to the U/Th-based Hulu2 time scale that may suffer from possibly significant variations in the "dead-carbon" effect of the Hulu Cave record over this period. The modeled time scale is a compromise between a fit to the varve counts and limiting the variability of the Hulu record dead-carbon fraction (Bronk Ramsey et al., 2012).

- The varve-counted Suigetsu record produces lower reservoir ages than IntCal09 or the age-modeled Suigetsu reference records, which are to be preferred following the definition of Sarnthein et al. (2007).

- When uncorrected ^{14}C concentrations are considered for corals of peak glacial to deglacial times, we find a single age range near 18.12–18.22 cal. ka, where a set of four corals displays slightly negative ^{14}C reservoir ages (Fairbanks et al., 2005) hardly exceeding 250 yr (as compared to ^{14}C age uncertainties of about 150–250 yr at 1σ). The "negative reservoir ages" of corals may be related to the coeval onset of pronounced oscillations in the fraction of modern carbon (FMC) during this time, which first affected the atmospheric ^{14}C signals and a little later the marine ^{14}C signals.
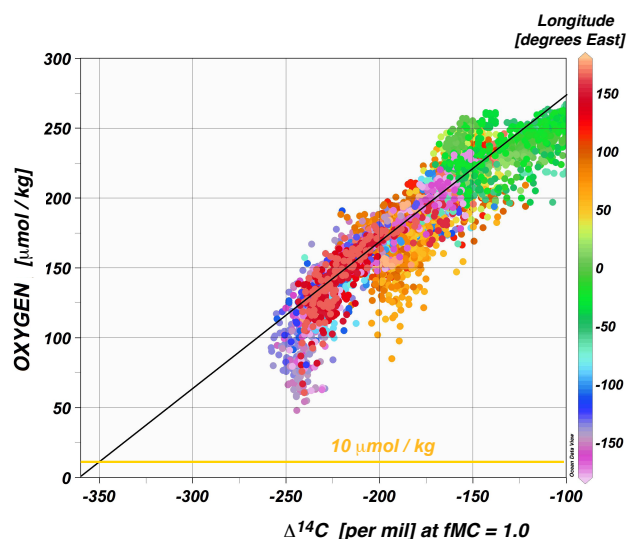

Fig. 5. Ratio of total dissolved oxygen (μmol kg^{-1}) vs. Δ^{14}C (equivalent to deep-water ventilation age) in the modern ocean below > 2000 m w.d. Positive O$_2$ "bump" at -140 to -170 per mil Δ^{14}C reflects the advection of freshly ventilated Weddell Sea waters. The regression line (average slope: 1.16 μmol kg^{-1} per ‰ Δ^{14}C) depicts the maximum O$_2$ averaged for each per mil of deep-water Δ^{14}C, that is for organic carbon flux rates below low-productivity regions. The line is extrapolated down to -360‰ Δ^{14}C for the maximum LGM deep-water age of 3600 yr shown in Fig. 7a. Enhanced O$_2$ depletion at -175 to -200 and -225 to -250‰ Δ^{14}C reflects increased flux rates of organic carbon below high productivity zones in the northern Indian and Pacific oceans each.

Comparison of the ^{14}C concentration measured in any sample with that calculated for Modern Carbon (MC) after decay over the independently determined age of the sample provides its original ^{14}C concentration, usually expressed in ‰ deviation from that of the modern standard. We use the ^{14}C concentrations of the atmosphere and deep ocean *during that time*, both expressed in a Modern Carbon (MC) fraction to translate ‰ Δ^{14}C values for intra-LGM, intra-HS-1, and intra-B/A into apparent age differences between the atmosphere and deep water (= benthic ventilation ages; ^{14}C yr). These are compared with related DIC, alkalinity, oxygen, PO$_4$, and CO$_3^{-2}$ estimates (Table 1; Figs. 2, 4–6).

In our study, the distribution patterns of ventilation ages are displayed for three glacial-to-deglacial time slices, the Δ^{14}C records of which rely on 10 to 12 core sites each (Table 1 and Fig. S1). Most of them occupy key locations in the ocean MOC, important for tracing the major deep-water masses. The age definitions largely follow Mix et al. (2001) for the LGM time slice (23–18 ka), Denton et al. (2006) and Sarnthein (2011) for HS-1 (17.5–14.7 ka), and the GICC05 age scale (Svensson et al., 2006) for the B/A (14.7–13.0 cal. ka).

Fig. 6. Past shifts in carbonate ion concentrations and tentative simplified circulation patterns below 1500 m w.d. (see caption of Fig. 7) for the B/A, HS-1, and LGM. Core locations and data sources are listed in Table 1. For the LGM we include [CO$_3^{-2}$] data derived by Yu et al. (2010) from B–Ca ratios (locations marked by + signs), which by and large corroborate our rough Δ^{14}C-based [CO$_3^{-2}$] pattern. Orange values and arrows mark concentrations higher than today, blue values and arrows present concentrations equal or lower than today (Fig. 1). Question marks earmark age estimates based on disputable dating techniques and/or indirect evidence (Table 1b and Supplement #8). Arrows are not based on real data, but on highly simplified inferences per analogy to those in Fig. 7. Hatched black arrows mark potential current of intermediate waters during HS-1. Red diamonds in the northeastern North Atlantic mark three sites with a composite Δ^{14}C record (Thornalley et al., 2011).

4 Deep-water ventilation ages and carbon absorption during LGM and deglacial times

4.1 Deep-water ventilation ages and glacial-to-deglacial changes in MOC

The gradients of fairly robust ^{14}C paleoventilation ages help to delineate some hypothetical patterns of deep-water circulation for the peak glacial and two deglacial scenarios (Table 1; Fig. 7). Age records from intermediate waters at less than 1500 m were ignored, because intermediate-water circulation tends to follow more small-scale and thus complex spatial variations, in several cases opposed to the trends of deep-water circulation (e.g., Pacific Δ^{14}C records of Duplessy et al., 1989, and Marchitto et al., 2007; Atlantic δ^{13}C transects of Curry and Oppo, 2005; Sarnthein et al., 1994).

Though fragmentary, the data sets listed in Table 1 at least are representative of three key regions for global MOC in the abyssal ocean, namely the North Atlantic onset and the North Pacific terminal region of the modern salinity conveyor belt, and the Atlantic sector of the Southern Ocean. Thus, the paleoreservoir age records do provide a sound first basis for large-scale interpolations, in particular, since LGM and B/A ages of deep waters display a remarkable regional and global homogeneity, except for the North Atlantic (because of small-scale longitudinal variations). By contrast, the fragmentary set of HS-1 ages does not yet display a consistent pattern, the main reason why we hesitate to assess a global average age for this time slice. In particular, the HS-1 circulation geometry may have been far more complex, consisting of several strongly competing sources of deep-water formation in the different hemispheres, sources that may have been subject to different levels of preformed nutrients.

The global trends in the distribution of deep-water ^{14}C ventilation ages reflect an LGM circulation geometry basically similar to today, as far as the prime sources and terminal regions of deep waters in the ocean are concerned. Also, we do not find any evidence that the LGM deep-ocean circulation pattern was essentially different, except for the Nordic Sea Overflow, the direction of which started to switch between modern and reversed HS-1-style orientation on millennial scales after 21 ka (Fig. S1a; Sarnthein et al., 2007). However, the relative densities, hence vertical position and flow strength of LGM deep waters, may have differed significantly from today (whereas Ritz et al., 2013, suggest a flow strength for LGM Atlantic MOC lower than but similar to the Holocene). In the Atlantic, these conclusions obtain independent support from δ^{13}C-based 3-D reconstructions of water mass-specific nutrient contents below 1500 m w.d. (Sarnthein et al., 1994; Curry and Oppo, 2005). Similar δ^{13}C evidence applies to the southwest Pacific, where most records of silt modal grain size suggest an LGM flow strength of deep waters similar to today (McCave et al., 2008).

Most striking is the widespread maximum of LGM ventilation ages in the deep Southern Ocean and North Pacific,

with values that exceed the modern reference level by 1100–1500 and up to > 2500 ^{14}C yr (Fig. 7a vs. numerical ranges in Fig. 1, Table 1, and Supplement #8). Most benthic age estimates were derived by accepting a highly variable ^{14}C reservoir age of surface waters, at several sites reaching up to 2500 ^{14}C yr. High planktic ages likewise arise from a direct tuning of ^{14}C ages to Greenland and Antarctic ice core chronologies (Thornalley et al., 2011; Skinner et al., 2010), from tephrochronology (Waelbroeck et al., 2001; E. Sikes, personal communication, 2012), from a comparison with the terrestrial Suigetsu record (Bronk Ramsey et al., 2012), and from the ^{14}C plateau technique (Fig. S1). This result challenges a little-substantiated but common dogma: that past surface waters had largely constant ventilation ages of ~ 400–500 Δ^{14}C yr, a value referring to the global modern average tentatively defined by Stuiver and Braziunas (1993) on the basis of ^{14}C ages of near-shore shells.

A record of the Southern Ocean LGM abyssal waters (Barker et al., 2010) shows a conflicting Δ^{14}C signature near 5000 m depth possibly much younger than that of overlying deep waters near 3800 m (Skinner et al., 2010). This signature would still be young if the Δ^{14}C estimates were modified by a distinct rise in planktic reservoir ages by > 1000 ^{14}C yr, equivalent to -120‰, which is far beyond the questionable value of 600 yr proposed as a constant by Barker et al. (2010). After all, these low benthic ages suggest a significant flow of glacial Antarctic-source waters that spread as rejuvenated AABW far north below "very old" northern-source deep waters into the Southern, Atlantic, and Indian Oceans (intersecting arrows in Fig. 7a and c).

During HS-1 the spatial distribution of ventilation ages was more complex (Fig. 7b), and clearly contrasted with both the LGM and modern patterns. On the one hand, upper deep waters that stemmed from LGM deep waters in the Southern Ocean (here already starting with ventilation ages of 2000–4000 ^{14}C yr) finally reached extreme, but highly variable ages of > 5000 ^{14}C yr in the "dead-end road" of the northeastern North Atlantic, ages that were totally unexpected prior to Thornalley et al. (2011). These old waters did not originate from southern-source intermediate waters (Burke and Robinson, 2012), but were overlain by somewhat younger intermediate waters found directly to the south and north of Iceland (Thornalley et al., 2011; Sarnthein et al., 2007; Fig. 7b). Obviously the stratification was linked to the salient meltwater stratification caused by the Heinrich-1 iceberg armadas (Sarnthein et al., 2001, and refs. cited therein). Like the records from the northeastern North Atlantic (Thornalley et al., 2011), the ^{14}C ventilation ages from the Icelandic Sea (PS2644) suggest that the deepwater circulation system was subject to basic oscillations, with 1000 yr pulses of rejuvenation (Icelandic Sea Modes 1 and 2).

On the other hand, Northeast Pacific deep-water ages then temporarily dropped to 1050 Δ^{14}C yr, equal to -122‰ (as compared to 2200 ^{14}C yr/-240‰ today) during HS-1, thus reflecting a ~ 1000 yr-long phase of major subpolar deep-
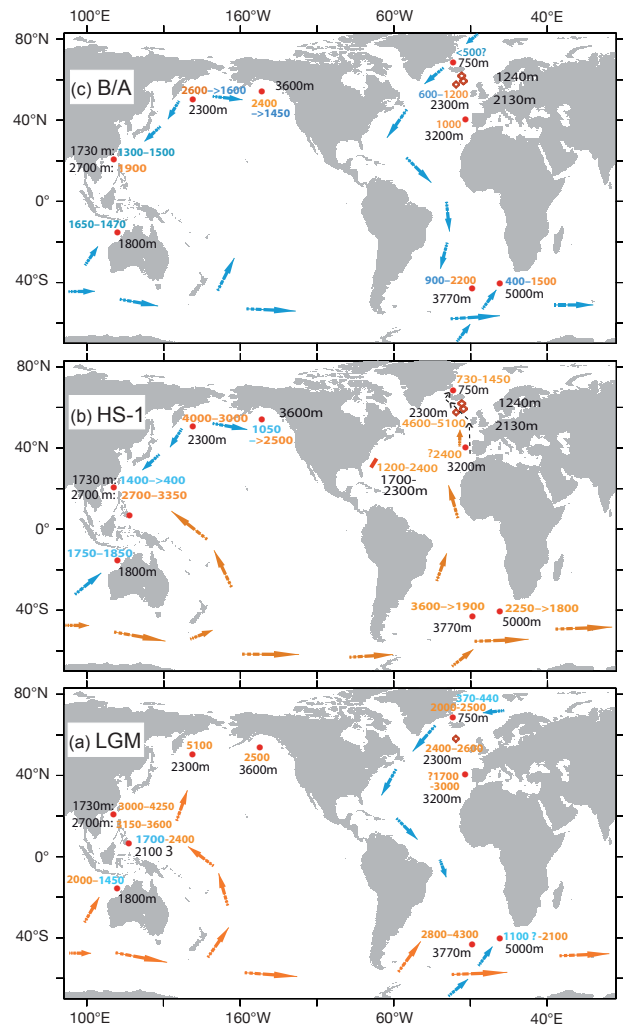

Fig. 7. Ranges of past ^{14}C ventilation ages (rounded) and tentative simplified circulation patterns below 1500 m w.d. (Sarnthein, 2011, modified). Arrows are not based on real data, but on highly simplified inferences per analogy to Fig. 1, based on a hypothesis of the ocean's circulation geometry and emanating from local benthic Δ^{14}C minima. In the Atlantic and off New Zealand, the arrows partly reflect gradients displayed in δ^{13}C transects for the Last Glacial Maximum (LGM), Heinrich-Stadial 1 (HS-1), and Bølling–Allerød (B/A) (Curry and Oppo, 2005; McCave et al., 2008; Sarnthein et al., 1994). Core locations and data sources are listed in Table 1. Orange values and arrows mark waters with ventilation ages higher than today, blue values and arrows present waters with ages equal or lower than today (Fig. 1). Intersecting arrows indicate Antarctic-source abyssal waters spreading below deep-ocean waters. Question marks earmark age estimates based on disputable dating techniques and/or indirect evidence (Table 1b and Supplement #8). Hatched black arrows mark potential current of intermediate waters during HS-1. Red diamonds in the northeastern North Atlantic show three sites with a composite Δ^{14}C record (Thornalley et al., 2011).

water convection down to 3600 m w.d. (Fig. S1h; Gebhardt et al., 2008, suppl., and Fig. S2). Lund et al. (2011) and Jaccard and Galbraith (2013, and preceding publications) most likely missed this event because of insufficient ^{14}C sampling resolution. Likewise, deep-water ages strongly dropped in the Southern Ocean, so far documented in the Atlantic and West Australian sectors (Skinner et al., 2010; Sarnthein et al., 2011). Altogether, the HS-1 deep ocean may have experienced a first major net rejuvenation after the LGM, linked to very short-lasting changes in the circulation geometry of the global conveyor belt.

In contrast to HS-1, low ventilation ages during the B/A suggest that the North Atlantic MOC had already returned to the modern mode (Fig. 7c). However, different from today, low ventilation ages of 1500 ^{14}C yr and less continued in the northern North Pacific from HS-1 over the B/A and reflected ongoing deep-water convection. Hence, the deglacial reversals in overturning circulation were not necessarily coupled at the Pacific and North Atlantic ends of the "global conveyor belt", a pattern still difficult to evaluate on the basis of our limited number of ventilation age records (also see Supplement #5).

4.2　A working hypothesis on carbon absorption in the LGM deep ocean

On the basis of the ages displayed in Fig. 7a and listed in Table 1, we now may derive a first rough estimate of the amounts of total carbon that could additionally be stored in the LGM deep ocean by extrapolating the regression between DIC and Δ^{14}C, displayed in Fig. 2a. The modern raw Δ^{14}C values cover an almost uniform range of -72 to -258 ‰ equivalent to $\sim$ 600–2400 ^{14}C yr with an arithmetic average of $\sim$ 1500 ^{14}C yr, equivalent to Δ^{14}C = -170 ‰ (Fig. 2a). As shown in Fig. 2b, we may likewise deduce a coarse arithmetic mean for our very fragmentary set of apparent peak glacial benthic ventilation ages ranging between 450 and $\sim$ 3600 ^{14}C yr (Table 1a). The LGM mean amounts to 2100 ^{14}C yr. In the deep ocean decay of peak glacial atmospheric ^{14}C over 2100 yr would produce a concentration of -230 ‰ Δ^{14}C relative to the peak glacial atmosphere (defined as "paleo-modern" atmosphere with Δ^{14}_{paleo}C = 0.0). The LGM mean transit time was $\sim$ 600 ^{14}C yr longer than today, a rise that suggests an increased LGM capacity of the deep ocean to absorb and store a large amount of additional carbon transferred from the atmosphere and terrestrial biosphere (Fig. 2c).

This conclusion is hardly hampered by a potential LGM rise in the flow rate of AABW as proposed by Campin et al. (1999). An increase in AABW flow would little affect our extrapolation of the DIC–age relationship to the past, since the regression slope of DIC vs. Δ^{14}C for modern AABW matches precisely that for NADW (GLODAP data in Fig. 2a). Moreover, the intercept of the Δ^{14}C–DIC relationship for AABW is slightly offset toward higher DIC

values (the "bump" in Fig. 2a), since most source waters of AABW are inherited from medium old "recycled" NADW, rejuvenated by $\sim$ 30 ‰ Δ^{14}C (see Sect. 2.2). Accordingly, AABW ab initio is far more carbon- and nutrient-enriched relative to a certain Δ^{14}C value than waters downwelled in the source regions of NADW. Thus we may infer that any LGM rise in the flow rate of AABW may shift the intercept of Δ^{14}C–DIC toward higher DIC values and imply a further rise in our conservative LGM DIC estimates for the global deep ocean. Similar trends will apply to the relationships of Δ^{14}C–POTALK, Δ^{14}C–PO$_4$, Δ^{14}C–O$_2$, and Δ^{14}C–CO$_3^{2-}$ (Table 1; Figs. 2, 4–6).

This hypothesis is supported by a vertical benthic δ^{13}C transect near New Zealand (McCave et al., 2008), where both LGM AABW at > 4000 m w.d. and overlying coeval derivates of NADW at $\sim$ 2000–3800 m w.d. are likewise nutrient-enriched by an equivalent of -1.25 ‰ $\Delta\delta^{13}$C vs. the Holocene. As a result of the LGM Circumpolar Current, the outlined stratification fits perfectly to that already identified in the Atlantic sector of the Southern Ocean (Figs. 2b and 7a), where LGM AABW with low ^{14}C ventilation ages forms an undercurrent at $\sim$ 5000 m below LGM NADW that is marked by high ages at $\sim$ 3800 m (Barker et al., 2010; Skinner et al., 2010).

By comparison with the modern Δ^{14}C average of -170 ‰ and the global arithmetic average of 2265 ± 40 µmol DIC kg^{-1} (Fig. 2a), a peak glacial Δ^{14}C of -230 ‰ (Fig. 2b) reflects an average DIC of 2350–2380 µmol kg^{-1} dissolved in the deep ocean, which implies a rise of 85–115 µmol kg^{-1} vs. today. In agreement with our working hypotheses outlined in Sect. 2.4, this range is based on the assumption of a largely constant global flux of organic and inorganic particulate carbon into the deep ocean, summing up to an average of 1.1 Gt C yr^{-1} (Fig. 2c).

In total, the LGM rise in DIC may correspond – disregarding the modern DIC–age relationship for the southern South Pacific (regression #5 in Fig. 2b) – to $\sim$ 730–980 Gt additional carbon stored in the global deep ocean below 2000 m w.d. This amount clearly exceeds the estimate of $\sim$ 530 Gt carbon (corresponding to an average deep-water aging by 325–440 ^{14}C yr) that sums up the Late-Holocene-to-glacial transfer of atmospheric 200 Gt carbon plus $\sim$ 330 Gt carbon derived from the terrestrial biosphere and soils (Monnin et al., 2001; Ciais et al., 2012).

Thus the potential LGM carbon storage of 730–980 Gt in the abyssal ocean, which accommodates the transfer from the atmosphere and biosphere, can also explain 200–450 Gt carbon most probably released from glacial Atlantic and Pacific intermediate waters, as suggested by benthic δ^{13}C and Δ^{14}C transects (Bryan et al., 2010; Burke and Robinson, 2012; Duplessy et al., 1989; Robinson et al., 2005; Rose et al., 2010; Curry and Oppo, 2005; Sarnthein et al., 1994). However, the number of robust ^{14}C ventilation ages from intermediate waters at less than 1500–2000 m is still too low and spotty in the three oceans to develop a more robust estimate of the overall

LGM carbon release from the complex layer of intermediate waters (Hain et al., 2011; Sarnthein, 2011).

In contrast to the LGM, a breakdown of glacial stratification of subpolar surface waters during HS-1 induced a massive and almost abrupt rejuvenation of deep waters in two key regions of the ocean. In the subpolar Northeast Pacific a transient sudden ~ 200 ‰ drop in the benthic-planktic ^{14}C offset (Gebhardt et al., 2008, and Figs. S1 and S2) suggests vigorous deep-mixing and deep-water formation down to > 3600 m w.d. from 17.4–16.0 ka (Fig. 7). This implies a major carbon release, evidence opposed to Jaccard and Galbraith (2012), who postulate a sustained stratification until the B/A on the basis of inadequately dated and resolved millennial-scale proxy records. Likewise, the Southern Ocean (Skinner et al., 2010) reflects a phase of enhanced vertical mixing during HS-1 and, in turn, a significant deglacial transfer of carbon back to the atmosphere and terrestrial biosphere (Crowley, 2011). Because of the unknown and possibly complex circulation system, we did not try to quantify the Δ^{14}C–DIC relationship for HS-1.

4.3 Implications for LGM oxygen content, alkalinity, and CaCO$_3$ dissolution

Figure 5 shows the large-scale overall trend of gradual oxygen depletion with increasing residence time (decreasing Δ^{14}C) of modern deep waters. This trend implies a considerable general drop in glacial deep-water O$_2$, locally inflated by enhanced flux rates of organic carbon. Assuming a general rise in O$_2$ solubility during the LGM (+20 µmol O$_2$ kg^{-1}; based on the same assumptions as outlined for the DIC transfer function), data listed in Table 1 show that the LGM deep Southern Ocean and the North Pacific basins may indeed have reached a suboxic O$_2$ level in bottom waters, assuming ~ 10 µmol O$_2$ kg^{-1} as the crucial boundary (Stramma et al., 2008). These estimates provide support for Boyle's (1988a and b) "nutrient deepening hypothesis" that implies a vertical shift in oxygen depletion from intermediate to deep-ocean waters. By and large, our estimates also agree with the patterns of Jaccard and Galbraith (2012). By contrast, during HS-1, O$_2$ dropped to zero in the northeast Atlantic only, a value effectively documented by rudimentary laminations in sediments at ~ 3060 m w.d. south of the Azores (core MD08-3180; H. Kinkel, personal communication, 2011).

Our Δ^{14}C-based conclusions on glacial-to-deglacial changes in the carbon sequestration of the deep ocean agree with various findings, trends, and concepts recently published on the basis of model simulations (Huiskamp and Meissner, 2012), marine-based Δ^{14}C records, and various other proxies. For example, combined evidence of benthic foraminiferal Δ^{14}C and boron / calcium ratios (Yu et al., 2010) suggests that > 100 Gt C were released from the deglacial deep ocean into the atmosphere during early deglacial times.

A significant rise in the residence time of deep waters probably led to an overall rise in CaCO$_3$ dissolution over the LGM (Archer et al., 2004). In addition to the prolonged effect of the biological pump (Fig. 2c), this scenario will supply further dissolved carbon and alkalinity to the abyssal ocean, as reflected in the regression slope of POTALK vs. Δ^{14}C (Fig. 4). This slope is 1 µmol kg^{-1} per ‰ Δ^{14}C, compared to a slope of 1.22 µmol kg^{-1} per ‰ Δ^{14}C for DIC vs. age (Fig. 2a). Hence the slope gradient of DIC vs. Δ^{14}C is steeper than that of POTALK. Since the absolute POTALK values are higher than DIC values (Figs. 2a vs. 4), the difference between POTALK and DIC, which approximates the carbonate ion concentration (CO$_3^{2-}$; Fig. 6), will progressively decrease with rising ^{14}C ventilation ages. Accordingly, a global LGM drop in deep-ocean CO$_3^{2-}$, which means more acidic deep waters, may lead in most ocean basins to a significant rise in glacial CaCO$_3$ dissolution (Fig. 6a), and thus to a further DIC rise beyond our conservative estimates on the basis of Fig. 2b.

Peak glacial CO$_3^{2-}$ concentrations (Fig. 6a) decreased by ~ 65 to more than 120 µmol kg^{-1} in the Atlantic, western Southern Ocean, and Pacific, however, by no more than ~ 0–65 µmol kg^{-1} in the eastern Indian Ocean and western North Atlantic, where dissolution hardly increased (Yu et al., 2010). Indeed, well-dated and highly resolved sediment records clearly suggest poor CaCO$_3$ preservation in both the deep northwestern and northeastern North Pacific (Gebhardt et al., 2008). These results contrast with the traditional view asserting a peak glacial maximum in Pacific CaCO$_3$ preservation. Possibly, the carbonate spikes widely noted for the LGM equatorial Pacific do actually belong to HS-1 and B/A (e.g., as classified by Anderson et al., 2008) in regions where (1) sedimentation rates hardly exceed 1.0–1.5 cm ky^{-1}, (2) past variations in planktic ^{14}C ventilation age are largely unknown, (3) benthic δ^{18}O records may lag behind the atmospheric records of climate change by up to 2000 yr (Duplessy et al., 1991b; Gebhardt et al., 2008), and (4) orbital age control is insufficient to resolve the age difference between the two intervals.

4.4 Outlook for changing carbonate dissolution over HS-1 and B/A – implications for changes in atmospheric Δ^{14}C

On the whole, the HS-1 abyssal ocean probably experienced a net rejuvenation of deep waters originating both in the northeastern North Pacific and, most likely, in the Southern Ocean (Gebhardt et al., 2008; details in Sect. 4.1 and Fig. 7b). This deglacial breakdown of bipolar surface water stratification was accompanied by a major bipolar release of carbon dioxide. Nevertheless, our data resolution does not yet allow an even rudimentary quantification of the overall MOC patterns, because they were more complex than during the LGM. A significant rise in CO$_3^{2-}$ concentrations in the eastern Indian and North Pacific oceans (~ 5–46 µmol kg^{-1};

Fig. 6) suggests a preservation spike of deep-water carbonate, which indeed is recorded in late HS-1 sediment sections (Gebhardt et al., 2008), in particular from the South China Sea (Miao and Thunnell, 1994), coeval with maximum dissolution in the northeast Atlantic. During the B/A (Fig. 7c), hardly any ^{14}C ventilation age of the abyssal ocean exceeds 2000 ^{14}C yr (Table 1). On the basis of Fig. 2, this significant general rejuvenation suggests a major drop in the carbon inventory of the deep ocean down to the modern level as early as during (late) HS-1. Our estimates of up to 730–980 Gt carbon released from the LGM deep ocean (Fig. 2b) exceed by far the pre-Bølling carbon transfer inferred from the ice core record of atmospheric CO_2 (Δ100 Gt C; Monnin et al., 2001), and hence may explain both a fast-growing biosphere uptake near the end of this interval and, most important, the 190 ‰ decrease in atmospheric Δ^{14}C over this interval (Bronk Ramsey et al., 2012). In contrast to Broecker and Barker (2007) and in agreement with Burke and Robinson (2012), we regard this Δ^{14}C drop as very consistent with the deglacial changes in carbon and ^{14}C content.

To arrive at this conclusion, we assume for simplicity (1) that atmospheric ^{14}C production remained constant over HS-1 (based on studies of ^{10}Be fluxes and paleomagnetic field strength; Muscheler et al., 2005, and Laj et al., 2004). (2) We calculate the effect of a transfer of the ^{14}C-depleted excess carbon (730–980 Gt DIC) from the LGM deep ocean to the LGM atmosphere during HS-1. (3) We consider that the LGM atmosphere contained 190 ppm CO_2 ($\sim$ 375 Gt C) with a ^{14}C concentration 1.4 times higher than that of the standard modern atmosphere (fMC) (Bronk Ramsey et al., 2012). The average apparent ventilation age of the LGM deep ocean of 2100 ^{14}C yr means that its ^{14}C concentration was 0.77 times that of the LGM atmosphere, and therefore 1.08 times that of the modern atmosphere (fMC). Our calculations include two further assumptions: (4) as outlined previously, the fragmentary DIC–Δ^{14}C data of deep waters, used in this study, can be employed for deriving coarse global arithmetic averages without knowing their approximate volumetric weighting. (5) Ocean intermediate waters took an active part in the atmosphere–biosphere–ocean carbon cycling as indicated by coeval Δ^{14}C and DIC changes, at least largely in a sense opposite to that of deep waters (Sects. 2.4 and 4.1).

Direct admixture of the excess abyssal carbon to the LGM atmosphere gives the following result: 375 Gt C · 1.4 fMC + 730 to 980 Gt C · 1.08 fMC add up to a mixture of 1105 to 1355 Gt C with a ^{14}C concentration of 1.19 to 1.17 fMC, which implies a deglacial 210 to 230 ‰ drop in atmospheric fMC. These values directly compare with 1.2 fMC recorded for the atmosphere during the early B/A (Bronk Ramsey et al., 2012) and indicate that the early B/A atmospheric Δ^{14}C, and hence the early deglacial 190 ‰ drop in atmospheric Δ^{14}C can indeed be reproduced by the admixture of ^{14}C-depleted carbon from the LGM deep ocean, a shift previously claimed to be a "mystery".

Atmospheric δ^{13}C records from Antarctic ice cores (Schmitt et al., 2012) provide further evidence for a major CO_2 outgassing from the deep ocean over HS-1. They show a negative 0.3 ‰ shift in $\delta^{13}C_{atm}$ that started around 17 ka, right near the onset of HS-1, perhaps marked by a slight overshoot signal, and continued until the B/A near 14.5 ka. In our point of view, the salient shift will not reflect a single 30 ppm pulse of carbon near 17 ka, but an ongoing small perturbation of the large ocean–atmosphere exchange by an input of ^{13}C-depleted, that is "old" CO_2, from both the deep Southern Ocean and subpolar North Pacific. This input of ^{13}C-depleted deep-ocean CO_2 initially lowered the δ^{13}C of the atmosphere and surface ocean until balanced by isotopic exchange between surface and intermediate waters, which led to a transient isotopic shift of atmospheric δ^{13}C. This balance was different from the state that had persisted over the preceding LGM and, later on, returned to a level comparable to the LGM over the Holocene. In our opinion this steady state was interrupted over $\sim$ 2500 yr until the B/A, likewise over the YD and Early Holocene, as long as the unusual net outgassing (Monnin et al., 2001) from the deep ocean continued. As soon as the outgassing ceased, the antecedent δ^{13}C level returned. The simple mass balance estimates above indicate that our suggested explanations are well within the possibilities of the system. Our reasoning considers the generally accepted ocean–atmosphere exchange of 90 Gt C yr^{-1} and fast equilibrations within the CO_2-bicarbonate system, which indicate that the transfer of CO_2 and isotopic equilibration within the carbonate system are not limiting factors. For example, average lifetimes of CO_2 range from only 27 s at 25 °C to 500 s at 0 °C (Vogel et al., 1970), and hence are irrelevant to the processes discussed in this study.

In reality, of course, the early B/A atmosphere contained only 240 ppm CO_2 ($\sim$ 475 Gt C), which means that more than 85 % (i.e., 630 to 880 out of 730 to 980 Gt) of the ^{14}C-depleted carbon released from the deep ocean was admixed from the atmosphere back into intermediate and surface waters of the ocean, over HS-1 also to the deep North Atlantic (Fig. 7), and a minor part to the terrestrial biosphere near the onset of B/A. Hence, we might expect a net increase in the carbon content of intermediate waters across HS-1 (e.g., in agreement with Δ^{14}C records of Bryan et al., 2010; Marchitto et al., 2007; Robinson et al., 2005; Sarnthein et al., 2007).

A thorough general circulation model study will be needed to simulate in detail the deglacial redistribution patterns of the ^{14}C-depleted carbon masses from the deep ocean pool up to the various carbon inventories of the ocean, bio- and atmosphere. Also, we will need to constrain more closely the differential capacity of the key regions in the deglacial deep ocean to sequester or release carbon from or into the atmosphere and terrestrial biosphere, in particular to establish a much denser network of 3-D paleoventilation-age transects both in the subpolar North Pacific and in the Southern Ocean.

In summary, we conclude that over HS-1 the upper deep waters of the abyssal ocean were subject to a distinct outgassing and early deglacial rejuvenation of an average of 600 ^{14}C yr and more. Based on our estimate, this was fully sufficient to account for a 190 permil drop in atmospheric Δ^{14}C over HS-1, which is also reflected in two major atmospheric ^{14}C plateaus (Sarnthein et al., 2007).

5 Conclusions

Extrapolating the validity of the modern global distributions of apparent ^{14}C ventilation ages and DIC, we propose a new working hypothesis to infer past changes in the carbon storage of ocean deep waters. On this basis of increased deep-water residence times, we tentatively conclude a potential rise in the LGM carbon inventory by approximately 730–980 Gt vs. pre-industrial times. This amount compares with an estimated glacial transfer of 530–700 Gt C from both the atmosphere and terrestrial biosphere in addition to a major DIC relocation from ocean intermediate waters down to > 2000 m w.d. A significant drop in ^{14}C ventilation ages during the early deglacial HS-1 suggests that a large portion of ^{14}C-depleted carbon was released from the deep ocean and cycled through the atmosphere and terrestrial biosphere. Accordingly, an alleged major "mystery" of last deglacial times, the source of ^{14}C-depleted additional atmospheric carbon, may have been unraveled.

The peak glacial deep ocean appears to have been a "cold acidic ocean", regionally with low O_2 concentrations, because of the prolonged residence time of deep waters, in agreement with the decreased LGM difference between potential alkalinity and DIC, in particular in the Atlantic and Pacific. This conjecture matches the glacial maximum in $CaCO_3$ dissolution for Atlantic sediments, particularly during HS-1, known since the first days of paleoceanography (Olausson, 1965; Berger, 1973). Our hypotheses call for major future studies. In particular, we see a need for well-focused model tests and a better reconstruction of LGM intermediate- and abyssal-water ventilation in the Southern Ocean, moreover, of the 3-D temporal and spatial patterns of carbonate dissolution.

Supplementary material related to this article is available online at http://www.clim-past.net/9/2595/2013/cp-9-2595-2013-supplement.pdf.

References

Adkins, J. F., Cheng, H., Boyle, E. A., Druffel, E. R. M., and Edwards, R. L.: Deep-sea coral evidence for rapid change in ventilation of the deep North Atlantic 15,400 years ago, Science, 280, 725–728, 1998.

Amante, C. and B. W. Eakins: ETOPO1 1 Arc-Minute Global Relief Model: Procedures, Data Sources and Analysis, NOAA Techn. Memorandum NESDIS NGDC-24, 19 pp., 2009.

Anderson, R. F., Fleisher, M. Q., Lao, Y., and Winckler, G.: Modern $CaCO_3$ preservation in equatorial Pacific sediments in the context of Late-Pleistocene glacial cycles, Mar. Chem., 111, 30–46, 2008.

Antia, A.N., Koeve, W., Fischer, G., Blanz, T., Schulz-Bull, D., Scholten, J., Neuer, S., Kremling, K., Kuss, J., Peinert, R., Hebbeln, D., Bathmann, U., Conte, M., Fehner, U., and Zeitzschel, B.: Basin-wide particulate carbon flux in the Atlantic Ocean: regional export patterns and potential for atmospheric CO_2 sequestration, Global Biogeochem. Cy., 15, 845–862, 2001.

Archer, D. and Winguth, A.: What caused the glacial/interglacial atmospheric pCO$_2$ cycles?, Rev. Geophys. 38, 159–189, 2000.

Archer, D., Martin, P., Buffett, B., Brovkin, V., Rahmstorf, S., and Ganopolski, A.: The importance of ocean temperature to global biogeochemistry, Earth Planet. Sci. Lett., 222, 333–348, 2004.

Bard, E.: Geochemical and geophysical implications of the radiocarbon calibration, Geochim Cosmochim A, 62, 2025–2038, 1998.

Barker, S., Knorr, G., Vautravers, M. J., Diz, P., and Skinner, L. C.: Extreme deepening of the Atlantic overturning circulation during deglaciation, Nature Geosci., 3, 567–571, doi:10.1038/NGEO921, 2010.

Basak, C., Martin, E. E., Horikawa, K., and Marchitto, T. M.: Southern Ocean source of ^{14}C-depleted carbon in North Pacific Ocean during the last deglaciation, Nature Geosci., 3, 770–774, 2010.

Berelson, W. M., Balch, W. M., Najjar, R., Feely, R. A., Sabine, C., and Lee, K.: Relating estimates of $CaCO_3$ production, export, and dissolution in the water column to measurements of $CaCO_3$ rain into sediment traps and dissolution on the sea floor: A revised global carbonate budget, Global Biogeochem. Cy., 21, GB1024, doi:10.1029/2006GB002803, 2007.

Berger, W. H.: Deep-sea carbonates. Pleistocene dissolution cycles, J. Foram. Res., 3, 187–193, 1973.

Berger, W. H. and Keir, R. S.: Glacial-Holocene changes in atmospheric CO_2 and the deep-sea record, AGU Geophys. Monogr., 29, 337–351, 1984.

Boyle, E. A.: The role of vertical chemical fractionation in controlling late Quaternary atmospheric carbon-dioxide, J. Geophys. Res.-Oceans 93, 15701–15714, 1988a.

Boyle, E. A.: Vertical oceanic nutrient fractionation and glacial interglacial CO_2 cycles, Nature 331, 55–56, 1988b.

Bronk Ramsey, C., Staff, R. A., Bryant, C. L., Brock, F., Kitagawa, H., van der Plicht, J., Schlolaut, G., Marshall, M. H., Brauer, A., Lamb, H. F., Payne, R. L., Tarasov, P. E., Haraguchi, T., Gotanda, K., Yonenobu, H., Yokoyama, Y., Tada, R., and Nakagawa, T.: A Complete Terrestrial Radiocarbon Record for 11.2 to 52.8 kyr B.P., Science, 338, 370–374, 2012.

Broecker, W. S.: Glacial-to-interglacial changes in ocean chemistry, Prog. Oceanogr., 11, 151–197, 1982.

Broecker, W. S.: The great ocean conveyor, Oceanography, 4, 79–89, 1991.

Broecker, W. and Barker, S. A.: 190‰ drop in atmosphere's Δ^{14}C during the 'Mystery Interval, Earth Planet. Sci. Lett., 256, 90–99, 2007.

Broecker W., Barker, S., Clark, E., Hajdas, I., Bonani, G., and Stott L.: Ventilation of the Glacial deep Pacific Ocean, Science, 306, 1169–1172, 2004.

Broecker, W., Clark, E., Barker, S., Hajdas, I., Bonani, G., and Moreno, E.: Radiocarbon age of late glacial deep waters from the equatorial Pacific, Paleoceanography, 22, PA2206, doi:10.1029/2006PA001359, 2007.

Bryan, S. P., Marchitto, T. M., and Lehman, S. J.: The release of ^{14}C-depleted carbon from the deep ocean during the last deglaciation: Evidence from the Arabian Sea, Earth Planet. Sci. Lett., 298, 244–254, 2010.

Burke, A. and Robinson, L. F.: The Southern Ocean's role in carbon exchange during the last deglaciation, Science, 335, 557–561, 2012.

Campin, J.-M., Fichefet, T., and Duplessy, J.-C.: Problems with unsing radiocarbon to infer ocean ventilation rates for past and present climates, Earth Planet. Sci. Lett., 165, 17–24, 1999.

Chase, Z., Anderson, R. F., Fleisher, M. Q., and Kubik, P. W.: Accumulation of biogenic and lithogenic material in the Pacific sector of the Southern Ocean during the past 40,000 years, Deep-Sea Res. II, 50, 799–832, 2003.

Ciais, P., Tagliabue, A., Cuntz, M., Bopp, L., Scholze, M., Hoffmann, G., Louranton, A., Harrison, S. P., Prentice, I. C., Kelley, D. I., Koven, C., and Piao, S. L.: Large inert carbon pool in the terrestrial biosphere during the Last Glacial Maximum, Nature Geoscience, 5, 74–79, 2012.

Crowley, T. J.: Proximal trigger for late glacial Antarctic circulation and CO_2 changes, PAGES news, 19, 70–71, 2011.

Curry, W. B. and Oppo, D. W.: Glacial water mass geometry and the distribution of δ^{13}C of ΣCO_2 in the western Atlantic Ocean, Paleoceanography, 20, PA1017, doi:10.1029/2004PA001021, 2005.

Denton, G. H., Broecker, W. S., and Alley, R. B.: The Mystery Interval 17.5–14.5 kyrs ago, PAGES News, 14, 14–16, 2006.

Duplessy, J.-C., Arnold, M., Bard, E., Juillet-Leclerc, A., Kallel, N., and Labeyrie, L.: AMS ^{14}C study of transient events and of the ventilation rate of the Pacific intermediate water during the last deglaciation, Radiocarbon, 31, 493–502, 1989.

Duplessy, J.-C., Labeyrie, L., Juillet-Leclerc, A., Maitre, F., Duprat, J., and Sarnthein, M.: Surface salinity reconstruction of the North Atlantic Ocean during the Last Glacial Maximum, Ocean. Acta, 14, 311–324, 1991a.

Duplessy, J.-C., Bard, E., Arnold, M., Shackleton, N. J., Duprat, J., and Labeyrie, L. D.: How fast did the ocean-atmosphere system run during the last deglaciation?, Earth Planet. Sci. Lett., 103, 27–40, 1991b.

Fairbanks, R. G., Mortlock, R. A., Chiu, T.-C., Cao, L., Kaplan, A., Guilderson, T. P., Fairbanks, T. W., Bloom, A. L., Grootes, P. M., and Nadeau, M. J.: Radiocarbon calibration curve spanning 0 to 50,000 years BP based on paired 130Th/234U/238U and 14C dates on pristine corals, Quaternary Sci. Rev., 24, 1781–1796, 2005.

Franke, J., Schulz, M., Paul, A., and Adkins, A. F.: Assessing the ability of the ^{14}C projection-age method to constrain the circulation of the past in a 3-D ocean model, Geochem. Geophys. Geosyst., 9, Q08003, doi:10.1029/2008GC001943, 2008.

Gebhardt, H., Sarnthein, M., Kiefer, T., Erlenkeuser, H., Schmieder, F., and Röhl, U.: Paleonutrient and paleoproductivity records from the subarctic North Pacific for Pleistocene glacial terminations I to V, Paleoceanography, 23, PA4212, doi:10.1029/2007PA001513, 2008.

Hain, M. P., Sigman, D. M., and Haug, G. H.: Shortcomings of the isolated abyssal reservoir model for deglacial radiocarbon changes in the mid-depth Indo-Pacific Ocean, Geophys. Res. Lett., 38, L04604, doi:10.1029/2010GL046158, 2011.

Huiskamp, W. N. and Meissner, K. J.: Oceanic carbon and water masses during the Mystery Interval: A model-data comparison study, Paleoceanography, 27, PA4206, doi:10.1029/2012PA002368, 2012.

Jaccard, S. L. and Galbraith, E. D.: Large climate-driven changes of oceanic oxygen concentrations during the last deglaciation, Nature Geoscience, 5, doi:10.1038/ngeo1352, 2012.

Jaccard, S. L. and Galbraith, E. D.: Direct ventilation of the North Pacific did not reach the deep ocean during the last deglaciation, Geophys. Res. Lett., 40, 199–203, doi:10.1029/2012GL054118, 2013.

Key, R. M., Kozyr, A., Sabine, C. L., Lee, K., Wanninkhof, R., Bullister, J. L., Feely, R. A., Millero, F. J., Mordy, C., and Peng, T.-H.: A global ocean carbon climatology: Results from Global Data Analysis Project (GLODAP), Global Biogeochem. Cy., 18, GB4031, doi:10.1029/2004GB002247, 2004.

Laj, C., Kissel, C., and Beer, J.: High resolution global paleointensity stack since 75 kyr (GLOPIS-75) calibrated to absolute values, in: Timescales of the Paleomagnetic Field, Amer. Geophys. Union Monographs, 145, 255–265, 2004.

Lund, D. C., Mix, A. C., and Southon, J.: Increased ventilation age of the deep northeasst Pacific Ocean during the last deglaciation, Nature Geoscience, 4, 771–774, doi:10.1038/ngeo1272, 2011.

Marchitto, T., Lehman, S., Ortiz, J., Fluckiger, J., and van Geen, A.: Marine radiocarbon evidence for the mechanism of deglacial atmospheric CO_2 rise, Science, 316, 1456–1459, 2007.

Matsumoto, K.: Radiocarbon-based circulation age of the world oceans, J. Geophys. Res., 112, C09004, doi:10.1029/2007JC0040952007, 2007.

McCave, I. N., Carter, l., and Hall, I. R.: Glacial-interglacial changes in water mass structure and flow in the SW Pacific Ocean, Quat. Sci. Rev., 27, 1886–1908, 2008.

Miao, Q. and Thunnell, R. C.: Glacial-Hoocene carbonate dissolution and sea surface temperatures in the South China and Sulu seas, Paleoceanography, 9, 269–290, 1994.

Mix, A. C, Bard, E., and Schneider, R.: Environmental processesof the Ice age: land, oceans, glaciers (EPILOG), Quatern. Sci. Rev., 20, 627–658, 2001.

Monnin, E., Indermühle, A., Dällenbach, A., Flückiger, J., Stauffer, B., Stocker, T. F., Raynaud, D., and Barnola, J.-M.: Atmospheric CO_2 concentrations over the last glacial termination, Science, 291, 112–114, 2001.

Muscheler, R., Beer, J., Kubik, P. W., and Synal, H.-A.: Geomagnetic field intensity during the last 60,000 years based on ^{10}Be and ^{36}Cl from the Summit ice cores and ^{14}C, Quatern. Sci. Rev., 24, 1849–1860, 2005.

Negre, C., Zahn, R., Thomas, A. L., Masque, P., Henderson, G. M., Martínez-Méndez, G., Hall, I. R., and Mas J. L.: Reversed flow of Atlantic deep water during the Last Glacial Maximum, Nature, 468, 84–88, 2010.

Olausson, E.: Evidence of climatic changes in North-Atlantic deep-sea cores with remarks on isotopic paleotemperature analysis, Prog. Oceanogr., 3, 221–252, 1965.

Orsi, A. H., Smethie, W. M., and Bullister, J. L.: On the total input of Antarctic waters to the deep ocean: A preliminary estimate from chlorofluorocarbon measur-ements., J. Geophys. Res.-Oceans, 107, 3122, doi:10.1029/2001JC000976, 2002.

Pflaumann, U., Sarnthein, M., Chapman, M., Funnell, B., Huels, M., Kiefer, T., Maslin, M., Schulz, H., Swallow, J., van Kreveld, S., Vautravers, M., Vogelsang, E., and Weinelt, M.: The glacial North Atlantic: Sea surface conditions reconstructed by GLAMAP-2000, Paleoceanography, 18, 1–28, doi:10.1029/2002PA000774, 2003.

Rahmstorf, S.: Thermohaline ocean circulation, Encyclopedia of Quaternary Sciences, Elsevier, 1–10, 2006.

Raven, J. A. and Falkowski, P. G.: Oceanic sinks for atmospheric CO_2, Plant Cell Environ., 22, 741–755, 1999.

Redfield, A. C., Ketchum, B. H., and Richards, F. A.: The influence of organisms on the composition of sea-water, 26–77, in: The Sea, Hill, M. N., Vol.2, 554 pp., John Wiley & Sons, New York, 1963.

Reimer, P. J., Baillie, M. G. L., Bard, E., Bayliss, A., Beck, J. W., Blackwell, P. G., Bronk Ramsey, C., Buck, C. E., Burr, G. S., Edwards, R. L., Friedrich, M., Grootes, P. M., Guilderson, T. P., Hajdas, I., Heaton, T. J., Hogg, A. G., Hughen, K. A., Kaiser, K. F., Kromer, B. McCormac, F. G., Manning, S. W., Reimer, R. W., Richards, D. A., Southon, J. R., Talamo, S., Turney, C. S. M., van der Plicht, J., and Weyhenmeyer, C. E.: INTCAL09 and MARINE09 radiocarbon age calibration curves, 0–50,000 years cal. BP, Radiocarbon, 51, 1111–1150, 2009.

Reimer, P. J., Bard, E., Bayliss, A., Beck, J. W., Blackwell, P. G., Bronk Ramsey, C., Buck, C. E., Cheng, H., Edwards, R. L., Friedrich, M., Grootes, P. M., Guilderson, T. P., Hajdas, I., Hatté, C., Heaton, T. J., Hoffmannm, D. I., Hogg, A. G., Hughen, K. A., Kaiser, K. F., Kromer, B., Manning, S. W., Niu, M., Reimer, R. W., Richards, D. A., Scott, E. M., Southon, J. R., Staff, R. A., Turney, C. S. M., and van der Plicht, J.: INTCAL13 and MARINE13 radiocarbon age calibration curves, 0–50,000 years cal. BP, Radiocarbon, 55, 1869–1887, 2013.

Ritz, S. P., Stocker, T. F., Grimalt, J. O., Menviel, L., and Timmermann, A.: Estimated strength of the Atlantic overturning circulation during the last deglaciation, Nature geoscience, 6, 208–212, doi:10.1038/NGEO1723, 2013.

Robinson, L., Adkins, J. F., Keigwin, L. D., Southon, J., Fernandez,D. P., Wang, S.-L., and Scheirer, D. S.: Radiocarbon variability in the western North Atlantic during the last deglaciation, Science, 310, 1469–1473, 2005.

Rose, K. A., Sikes, E. L., Guilderson, T. P., Shane, P., Hill, T. M., Zahn, R., and Spero, H. J.: Upper-ocean-to atmosphere radiocarbon offsets imply fast deglacial carbon dioxide release, Nature, 466, 1093–1097, 2010.

Sarnthein, M.: Northern meltwater pulses, CO_2 and Atlantic ocean convection, Science, 331, 156–158, 2011.

Sarnthein, M., Winn, K., Jung, S., Duplessy, J. C., Labeyrie, L., Erlenkeuser, H., and Ganssen, G.: Changes in East Atlantic deep-water circulation over the last 30,000 years – An eight-time-slice record, Paleoceanography, 9, 209–267, 1994.

Sarnthein, M., Stattegger, K. , Dreger, D. , Erlenkeuser, H., Grootes, P., Haupt, B., Jung, S., Kiefer, T., Kuhnt, W., Pflaumann, U., Schäfer-Neth, C., Schulz, H., Schulz, M., Seidov, D., Simstich, J., van Kreveld-Alfane, S., Vogelsang, E., Völker, A., and Weinelt, M.: Fundamental modes and abrupt changes in North Atlantic circulation and climate over the last 60 ky – Concepts, reconstruction, and numerical modelling, in: The northern North Atlantic: A changing environment, edited by: Schäfer, P., Ritzrau, W., Schlüter, M., and Thiede, J., Springer, 365–410, 2001.

Sarnthein, M., Grootes, P. M., Kennett, J. P., and Nadeau, M.-J.: ^{14}C reservoir ages show deglacial changes in ocean currents and carbon cycle, AGU Geophys. Monogr., 173, 175–196, 2007.

Sarnthein, M., Grootes, P. M., Holbourn, A., Kuhnt, W., and Kühn, H.: Tropical warming in the Timor Sea led deglacial Antarctic warming and almost coeval atmospheric CO_2 rise by > 500 yr, Earth Planet. Sci. Lett., 302, 337–348, 2011.

Schlitzer, R.: Carbon export fluxes in the Southern Ocean: results from inverse modelling and comparison with satellite-based estimates, Deep Sea Res. II, 49, 1623–1644, doi:10.1016/S0967-0645(02)00004-8, 2002.

Schmitt, J., Schneider, R., Elsig, J., Leuenberger, D., Lourantou, A., Chappellaz, J., Köhler, P., Joos, F., Stocker, T. F., Leuenberger, M., and, Fischer, H.: Carbon isotope constraints on the deglacial CO_2 rise from ice cores, Science, 23, 711–714, doi:10.1126/science.1217161, 2012.

Schneider, B., Schlitzer, R., Fischer, G., and Nöthig, E.-M.: Depth-dependent elemental compositions of particulate organic matter (POM) in the ocean, Global Biogeochem. Cy., 17, 1032–1047, doi:10.1029/2002GB001871, 2003.

Sigman, D. M. and Boyle, E.: Glacial/interglacial variations in atmospheric carbon dioxide, Nature, 407, 859–869, 2000.

Sigman, D. M., Hain, M. P., and Haug, G. H.: The polar ocean and glacial cycles in atmospheric CO_2 concentration, Nature, 466, 47–55, 2010.

Skinner, L. C.: Glacial-interglacial atmospheric CO_2 change: a possible "standing volume" effect on deep-ocean carbon sequestration, Clim. Past, 5, 537–550, doi:10.5194/cp-5-537-2009, 2009.

Skinner, L. C., Fallon, S., Waelbroeck, C., Michel, E., and Barker, S.: Ventilation of the deep Southern Ocean and deglacial CO_2 rise, Science, 328, 1147–1151, 2010.

Stommel, H.: Thermohaline convection with two stable regimes of flow, Tellus, 13, 224–230, 1961.

Stramma, L., Johnson, G. C., Sprintall, J., and Mohrholz, V.: Expanding oxygen-minimum zones in the tropical oceans, Science, 320, 655–658, 2008.

Stuiver, M. and Braziunas, T. V.: Modeling atmospheric ^{14}C influences and ^{14}C ages of marine samples to 10,000 B.C., Radiocarbon, 35, 137–189, 1993.

Svensson, A., Andersen, K. K., Bigler, M., Clausen, H. B., Dahl-Jensen, D., Davies, S. M., Johnsen, S. J., Muscheler, R., Rasmussen, S. O., Röthlisberger, R., Steffensen, J. P., and Vinther, B. M.: The Greenland Ice Core Chronology 2005, 15–42 ka. Part 2: comparison to other records, Quatern. Sci. Rev., 25, 3258–3267, 2006.

Tagliabue, A., Bopp, L., Roche, D. M., Bouttes, N., Dutay, J.-C., Alkama, R., Kageyama, M., Michel, E., and Paillard, D.: Quantifying the roles of ocean circulation and biogeochemistry in governing ocean carbon-13 and atmospheric carbon dioxide at the last glacial maximum, Clim. Past, 5, 695–706, doi:10.5194/cp-5-695-2009, 2009.

Thiede, J.: Wind regimes over the late Quaternary southwest Pacific Ocean, Geology, 7, 259–262, 1979.

Thornalley, D. J. R., Barker, S., Broecker, W. S., Elderfield, H., and McCave, I. N.: The deglacial evolution of the North Atlantic deep convection, Science 331, 202–205, 2011.

Voelker, A.: Zur Deutung der Dansgaard-Oeschger Ereignisse in ultrahoch auflösenden Sedimentprofilen aus dem Europäischen Nordmeer, D.Sc. Thesis, 1–180, Univ. of Kiel, Kiel, Germany, 1999.

Vogel, J. C., Grootes, P. M., and Mook, W. G.: Isotopic fractionation between gaseous and dissolved carbon dioxide, Z. Physik, 230, 225–238, 1970.

Waelbroeck, C., Duplessy, J.-C., Michel, E., Labeyrie, L., Paillard, D., and Duprat, J.: The timing of the last deglaciation in North Atlantic climate records, Nature, 412, 724–727, 2001.

Weinelt, M., Vogelsang, E., Kucera, M., Pflaumann, U., Sarnthein, M., Voelker, A., Erlenkeuser, H., and Malmgren, B. A.: Variability of North Atlantic heat transfer during MIS 2, Paleoceanography, 18, PA1071, doi:10.1029/2002PA000772, 2003.

Yu, J., Broecker, W. S., Elderfield, H., Jin, Z., McManus, J., and Zhang, F.: Loss of carbon from the deep sea since the last glacial maximum, Science, 330, 1084–1087, 2010.